Characterization of the pregnane X receptor (PXR) from European hake (*Merluccius merluccius*): cloning, ligand activation, and bioinformatical analyses

This thesis is submitted in partial fulfilment of the requirements for the degree of Master of Science

By Karoline Nedrebø

Department of Biological Sciences
Faculty of Mathematics and Natural Science
UNIVERSITY OF BERGEN

September 2022

Acknowledgements

This master thesis was funded by the Research Council of Norway and has been part of the iCod 2.0 project (project no. 244564) and dCod 1.0 project (project no. 248840).

First and foremost, I would like to express my greatest gratitude to my supervisors Odd André Karlsen and Anders Goksøyr. Thank you both for your enthusiasm, help, and support throughout this year. Thank you for showing great interest in my work both in the laboratory and in the writing process, by giving me encouragement and sharing your wisdom.

Next, I would like to thank Rhîan Gaenor Jacobsen for teaching me and helping me in the lab. Your encouragement and support meant the world, and you were always available to help when needed. I would also like to thank the remaining members of the environmental toxicology group, including fellow students, for always providing a supportive environment and partaking in interesting discussion over the lunch table.

Finally, I would like to thank my friends, family, and boyfriend for the unvaluable support and patients, for showing interest and trying to understand what I have been working on this year.

Nærbø, september 2022
Karoline Nedrebø

Abstract

As a response to adverse environmental conditions, organisms have throughout evolution generated a collection of gene families and pathways providing protection and repair of damage caused by physical, chemical, and biological stressors (the defensome). A network of genes and diverse metabolic pathways comprise the chemical defensome, which allows the organism to detect diverse compounds and orchestrate a defense against the potentially toxic chemicals. The chemical defense system constitutes efflux transporters transporting compounds out of the cells when they enter and after they have been metabolized (Phase 0 and III), detoxifying enzymes that transform compounds to inactive- or more easily eliminated metabolites (Phase I-II), and soluble receptors and ligand-activated transcription factors that function as sensors of diverse compounds. The pregnane X receptor (PXR) is a ligand-activated transcription factor belonging to the nuclear receptor (NR) superfamily, and it is also known as NRI12. PXR is activated by a variety of ligands, including both endobiotic and xenobiotic compounds, and subsequently regulates the expression of different genes involved in biotransformation (transporters, CYP genes, genes encoding conjugating and reducing enzymes) as a response to the detected compound. As PXR constitute an important role as xenosensor, and an essential member of the chemical defensome, more studies have focused on its ligand-binding properties and function as a regulator of stress in different species. Interestingly, a recent study reported the loss of *pxr* in most of the species belonging to the *Gadiformes* order, including Atlantic cod (*Gadus morhua*), however, the *pxr* gene was apparently retained in the European hake (*Merluccius merluccius*). This raises interesting questions from an evolutionary and toxicological perspective, regarding the physiological role and function of PXR in European hake. This study aimed to characterize PXR in the European hake on a molecular and functional level by performing primary structure- and phylogenetic analysis, and by assessing its potential transcriptional activation induced by different xenobiotics. This study provided supporting evidence that diverse changes to the *pxr* gene have occurred throughout evolution, and more closely related species were shown to have more similar PXR protein sequences (hake clustered with teleost fish in the phylogenetic three). Furthermore, *pxr* from hake was cloned and used to establish an *in vitro* luciferase gene reporter assay, where transcriptional activity of hakePXR was successfully induced by clotrimazole (known agonist for zebrafish PXR). Thus, this study provides important evidence for PXR functionality in European hake and suggest its role as a xenosensor is conserved in European hake.

List of Content

List of abbreviations

ABC	ATP-binding cassette
ADB	Agarose Dissolving Buffer
AF-1	activation function 1
AF-2	activation function 2
AHR	Aryl hydrocarbon receptor
AKR	Aldo-keto reductase
APS	Ammonium persulfate
BSA	Bovine serum albumin
CAR	Constitutive androstane receptor
CAT	Catalase
CCE	Carboxylesterase
cDNA	Complementary DNA
CYP	Cytochrome P450
D box	Distal box
DBD	DNA binding domain
DMEM	Dulbecco´s modified Eagle´s medium
DMSO	Dimethyl sulfoxide
DTT	DL-Dithiothreitol
E. coli	*Escherichia coli*
EDTA	Ethylenediaminetetraacetic acid
EPHX	Epoxide hydrolase
FBS	Fetal bovine serum
FMO	Flavin monooxygenase
GST	Glutathione-S-transferase
LB	Lysogeny Broth
LBD	Ligand binding domain
LBP	Ligand binding pocket
LOEC	Lowest observed effect concentration
LRA	Luciferase reporter gene assay
MCS	Multiple cloning site
NAT	*N*-acetyl transferase

NR	Nuclear receptor
NTD	N-terminal domain
ODV	Optical density volume
ONPG	*o*-Nitrophenyl β-D-galactopyranoside
PAS	Per-ARNT-Sim
PBS	Phosphate-buffered saline
PCR	Polymerase chain reaction
PMSF	Phenylmethylsulfonyl fluoride
PPAR	Peroxisome proliferator activated receptors
PTM	Post-translational modification
PXR	Pregnane X receptor
RAR	Retinoic acid receptors
ROS	Reactive oxygen specie
RT	Room temperature
SAP	Shrimp alkaline phosphatase
SDS	Sodium dodecyl sulfate
SDS-PAGE	Sodium-dodecyl-sulfate polyacrylamide gel electrophoresis
SOD	Superoxide dismutase
SULT	Sulfotransferase
SRC-1	steroid receptor coactivator 1
T_m	Melting temperature
TR	Thyroid hormone receptors
Tween 20	Opti-MEM® I reduced serum medium
	Polysorbate 20
UGT	UDP-glucuronosyl transferase
UV	Ultraviolet
zfPXR	Zebrafish PXR

1. Introduction

1.1 *The defense systems of organisms*

Adverse environmental conditions, as well as biological conditions, may impact cells and organisms as stress factors. As a response, organisms have throughout evolution generated a collection of gene families and pathways providing protection and repair of damage caused by physical, chemical, and biological stressors. Collectively, the genes and proteins providing such protection comprise an organisms "defensome" (Goldstone et al., 2006). The defensome's protective mechanisms can be further divided and classified into the "immune system" and the "chemical defensome" (Goldstone, 2008). The innate immune system is the first line of defense against biotic stressors such as pathogens, and it is fundamentally a two-tier system. One part of the system consists of specific surface receptors which interact with pathogens or pathogen-derived components, resulting in phagocyte activation (Miller et al., 2007). The second part of the immune system consists of direct opsonization, which is a process where opsonins (e.g., antibodies) tag foreign pathogens for elimination by phagocytes, and lysis of pathogens via the complement cascade (Miller et al., 2007; Thau, Asuka, & Mahajan, 2022). Another network of genes and diverse cellular pathways comprise the chemical defensome, which allows the organism to detect diverse compounds and orchestrate a defense against the potentially toxic chemicals. The defense system interacts with and metabolizes both exogenous chemicals (e.g., microbial products, heavy metals, phytotoxins, polycyclic aromatic hydrocarbons and halogenated organic compounds), endogenous signaling molecules (e.g., steroids), and endogenously generated compounds (e.g., reactive oxygen species (ROS), lipid peroxides, and heme degradation products) (Goldstone et al., 2006).

1.1.1 *The Chemical Defensome*

The chemical defense system is comprised of several diverse protein families which interact in different metabolic pathways to protect the cell (Figure 1), including: soluble receptors and ligand-activated transcription factors, biotransformation enzymes, efflux transporters, and antioxidant enzymes (Goldstone et al., 2006).

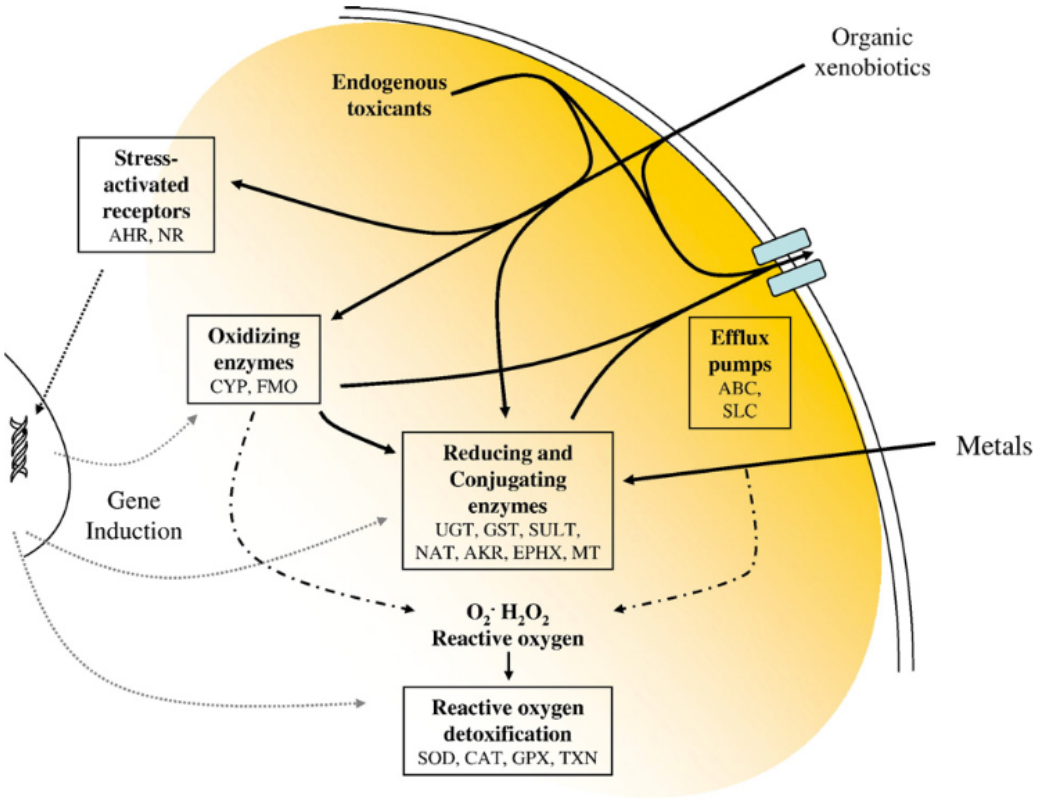

Figure 1. Organization of proteins and pathways constituting the chemical defensome. Toxicants are actively exported from the cell, as well as being subjected to a variety of biotransformative reactions. Solid lines indicate possible pathways for exogenous toxicants, dotted lines indicate possible gene induction as response to stress-activated receptors, and dot-dashed lines indicate possible source of toxicant-stimulated endogenous production of reactive oxygen. Illustration from Goldstone et al. (2006).

Efflux transporters such as ATP-binding cassette (ABC) proteins can be considered as both the first and the last line of cellular defense (Phase 0 and Phase III), since they both actively export toxicants out of the cell once they enter, as well as after the toxicants have been metabolized by enzymes in Phase I and II of the biotransformation (Dean, Hamon, & Chimini, 2001; Steinberg, 2012). Furthermore, when toxicants enter the cytoplasm, Phase I and II of biotransformation are often required to maintain biochemical homeostasis in the cell, by transforming the toxicants to inactive- or more easily eliminated metabolites (Goldstone, 2008; Steinberg, 2012). Phase I consists of oxidative, reductive, or hydrolytic transformation of toxic compounds (Steinberg, 2012). Oxidation is carried out by enzymes such as flavin monooxygenase (FMO) and cytochrome P450 (CYP), while reduction is carried out by enzymes such as aldo-keto reductases (AKRs). Hydrolysis reactions are carried out by e.g., epoxide hydrolases (EPHXs) and carboxylesterases (CCEs). Phase II consists of conjugative modifications of toxic compounds, most of which are already oxidized in Phase I, by glutathione-S-transferases (GSTs), sulfotransferases (SULTs), UDP-glucuronosyl transferases

(UGTs), and *N*-acetyl transferases (NATs) (De Marco et al., 2017; Sevior, Pelkonen, & Ahokas, 2012). However, biotransformation does not always result in less toxic compounds, and might generate reactive oxygen species (ROS) or other harmful metabolites. Exposure to ultraviolet (UV) radiation or normal metabolism can also lead to production of ROS. Therefore, genes encoding for antioxidant enzymes (e.g., superoxide dismutases (SODs), catalases (CATs), and peroxidases (GPXs and TXNs)) that protect the cell against both exogenous and endogenous ROS or other radicals are a critical part of the chemical defensome (De Marco et al., 2017; Goldstone et al., 2006).

As aforementioned, the chemical defensome also comprises soluble receptors and ligand-activated transcription factors. These nuclear receptors can function as sensors of chemical toxicants and include the protein family basic helix-loop-helix Per-ARNT-Sim (bHLH-PAS) and the nuclear receptor (NR) superfamily. Furthermore, the bHLH-PAS and NR protein families include ligand-activated transcription factors such as the aryl hydrocarbon receptor (AHR) and the pregnane X receptor (PXR), respectively. Both the AHR and the PXR are activated by a variety of chemicals, and subsequently regulates the expression of different genes involved in biotransformation (transporters, CYP genes, genes encoding conjugating and reducing enzymes) as a response to the detected compound (Timme-Laragy, Cockman, Matson, & Di Giulio, 2007; Wada, Gao, & Xie, 2009).

1.2 *The Nuclear Receptor superfamily*

Nuclear receptors (NRs) constitute a large superfamily of evolutionary related transcription factors. All NR proteins share a similar modular structure comprised of five functional domains, including the DNA binding domain (DBD) and the ligand binding domain (LBD). DBD and LBD might be valued as the most important domains for receptor function, which is reflected by the high conservation of these domains among NRs belonging to different subfamilies (Germain, Staels, Dacquet, Spedding, & Laudet, 2006). However, differences in the structural domains of NRs allow them to regulate a wide range of pathways involved in physiological processes of the cell, such as development, growth, procreation, cell differentiation, proliferation, apoptosis, and the maintenance of homeostasis. Additionally, as activation of most NRs are ligand-dependent, they have become evident pharmacological targets. Some pharmaceuticals targeting NRs include contraception pills, anti-inflammatory

drugs, and medicaments used for treatment of various diseases such as diabetes, skin diseases, hormone resistance syndromes, and some cancers. (Renaud & Moras*, 2000).

NRs are generally activated by small lipid-soluble molecules, including steroid hormones (e.g., estrogen and progesterone), retinoic acid, oxysterols, vitamins, eicosanoids, bile acids and thyroid hormones (Renaud & Moras*, 2000; Sever & Glass, 2013). Moreover, some NRs are also involved in detection and coordination of metabolism of diverse xenobiotics (including toxicants), and can be referred to as xenosensors (Pascussi et al., 2008). As contrast to most intercellular signal molecules, that interact with cell surface receptors, NR ligands can cross the cell membrane and directly interact with NRs within the cell (Sever & Glass, 2013). Once ligand-binding to an NR occurs, the receptor undergoes conformational changes into an active state. Depending on the type of NR and the ligand bound, the receptor will either form monomers, homodimers, or heterodimers and bind to specific regulatory DNA sequences of their target genes (Pascussi et al., 2008; Sever & Glass, 2013). If ligand-binding to receptor results in transcriptional activation of a target gene, the ligand is referred to as an agonist. Conversely, if ligand-binding of a receptor leads to transcriptional repression (inactivation) of target gene, the ligand is referred to as an antagonist (Pascussi et al., 2008).

Furthermore, based on sequence and structural similarities, and both ligand- and DNA binding features, NRs can be divided into seven subfamilies: NR0, NR1, NR2, NR3, NR4, NR5 and NR6 (Figure 2). NR1 is the largest subfamily and comprises nuclear receptors that are regulated by various lipophilic ligands such as thyroid hormones, fatty acids, and sterols. Nuclear receptors of the NR1 subfamily include thyroid hormone receptors (TR), retinoic acid receptors (RAR), peroxisome proliferator activated receptors (PPAR), pregnane X receptors (PXR), and others (Weikum, Liu, & Ortlund, 2018).

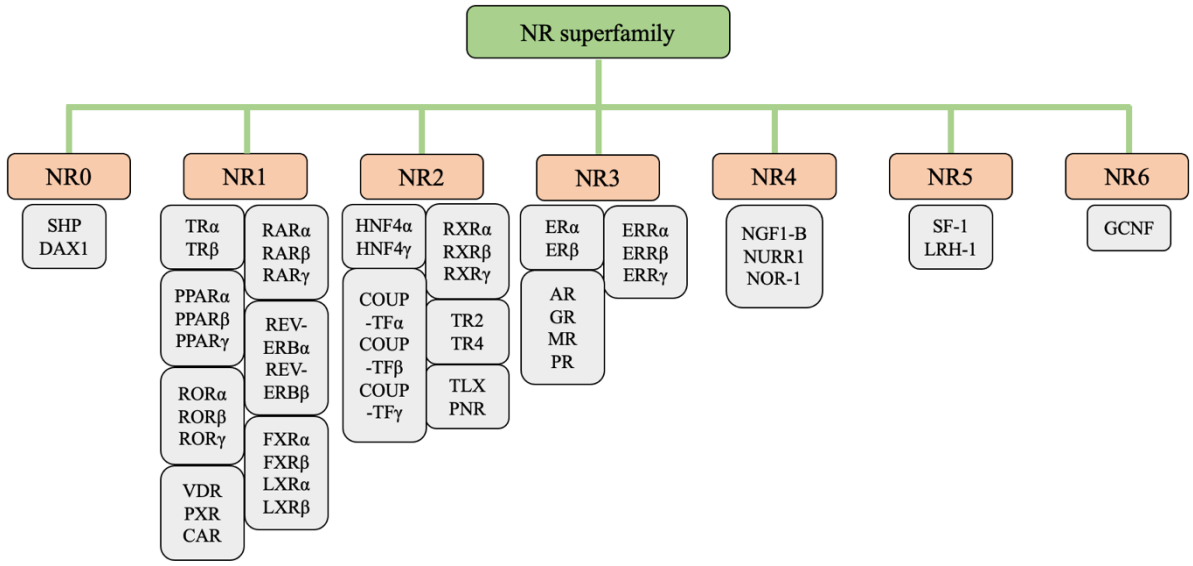

Figure 2. The nuclear receptor superfamily. Overview of the NR superfamily, highlighting the seven NR subfamilies and the individual NRs divided into groups within the subfamilies (Weikum et al., 2018).

1.3 *Pregnane X Receptor*

The pregnane X receptor (PXR) is a member of the NR superfamily, it belongs to group I within the subfamily NR1, and is referred to as NR1I2 (Weikum et al., 2018). PXR is activated by a variety of ligands, including both endobiotic and xenobiotic compounds, and is a regulator of xenobiotic detoxification enzymes (phase I-III). Hence, PXR is an important xenosensor and regulator of adaption to chemical stress (Kretschmer & Baldwin, 2005).

1.3.1 *Signaling, interaction partners, and functional roles of PXR*

As mentioned earlier, NRs form monomers, homodimers, or heterodimers in their active state. Once a ligand binds to PXR, the receptor is activated and it translocate to the nucleus where it forms a heterodimer with the retinoid X receptor (RXR) (Timsit & Negishi, 2007). The heterodimer complex further regulates a response to the ligand by binding to response elements present in the promoter regions of drug-metabolizing enzymes (e.g., Phase I CYP3A, CYP2B, CYP2C or Phase II conjugating enzymes) and transporter genes (e.g., MRP2, OATP2, or MDR1) (Figure 3) (Wada et al., 2009).

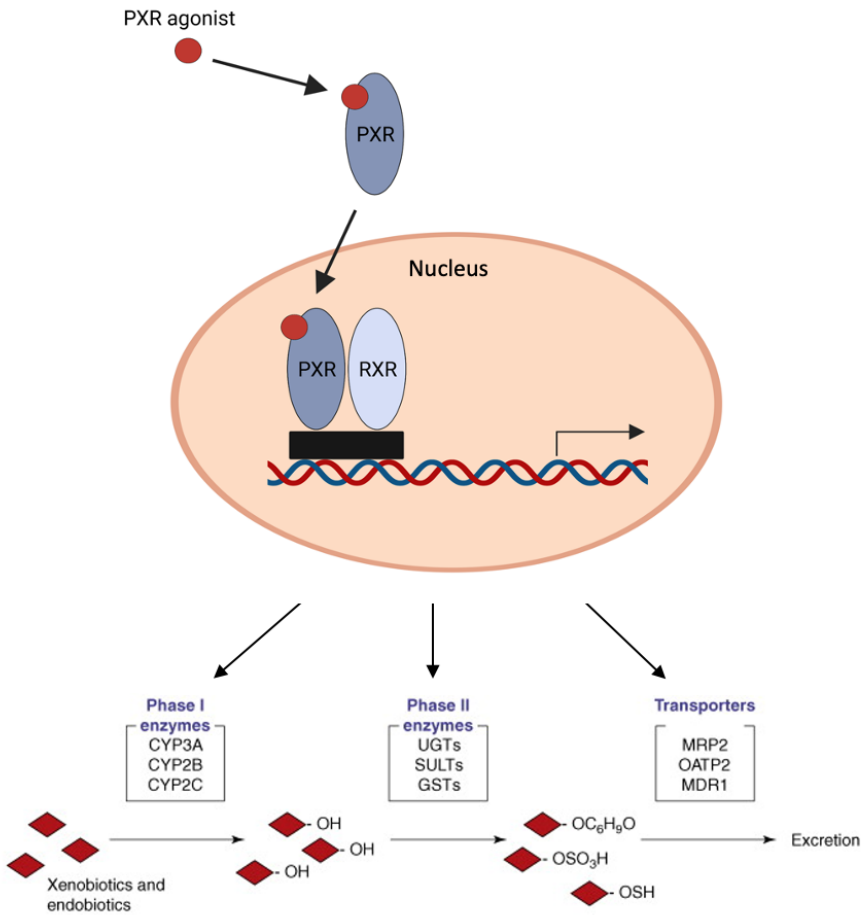

Figure 3. PXR mechanism of action. After activation of PXR by ligand (agonist)-biding in cytosol, PXR translocate to the nucleus where it forms a heterodimer complex with RXR. The heterodimer complex binds to response elements of target genes and activate transcription of detoxification enzymes and transporters (Phase I-III). The illustration is created with biorender.com and is adapted from Wada et al. (2019).

However, the activation of PXR and subsequent induction of target genes are not solely dependent on formation of a heterodimer, but also the ligand bound and co-regulators. PXR is originally located in the cytosol, where it is complexed with and silenced by a corepressor. Once ligand binding of PXR occurs, a coactivator (e.g., steroid receptor coactivator 1 (SRC-1)) takes the place of the corepressor, and the activated PXR forms a heterodimer with a RXR and induces gene transcription in the nucleus (Wang et al., 2008).

1.3.2 *PXR functional domains and protein structure*

Like most members of the NR superfamily, PXR have a modular protein structure with five functional domains (di Masi, Marinis, Ascenzi, & Marino, 2009). These domains are the N-terminal domain (A/B), the DNA binding domain (C), the hinge region (D), and the ligand binding domain (E) (Figure 4) (Weikum et al., 2018).

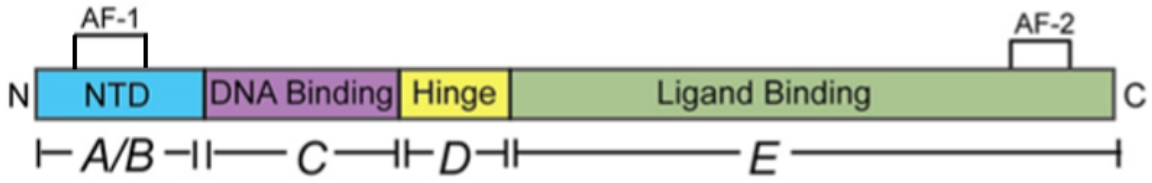

Figure 4. Structural representation of PXR and its functional domains. The five functional domains constituting PXR are: A/B) the N-terminal domain, C) the DNA binding domain, D) the hinge-region, E) and the ligand binding domain. Activation function 1 and 2 (AF-1 and AF-2) are also indicated. The illustration is adapted from Weikum et al. (2018).

The N-terminal domain (NTD) is a highly disordered and poorly conserved domain, which contains the activation function 1 (AF-1). AF-1 interacts with several co-regulators in a cell- and promoter-specific manner. Also, the NTD site is a target for various post-translational modifications (PTMs) such as phosphorylation and acetylation, leading to increase or decrease in transcriptional activity of the receptor (Weikum et al., 2018).

The DNA binding domain (DBD) is the most conserved domain amongst NRs, and it consists of two subdomains. Each subdomain contains a DNA-binding zinc finger motif, followed by an amphipathic helix and a peptide loop. The first domain interacts with the major groove through the DNA-reading helix to make base-specific interactions with response elements (specific DNA sequences). The second subdomain helix interacts with the DNA backbone in a non-specific manner. In addition, the peptide loop of the second subdomain is involved in DBD dimerization, as it contains the distal box (D box) (Weikum et al., 2018).

The hinge region is poorly conserved, regarding both sequence identity and length. This region is a short and flexible link between the DBD and LBD, and it is a site for PTMs. Also, the hinge region can contain a nuclear localization signal (Weikum et al., 2018).

The ligand binding domain (LBD) is a moderately conserved domain that acts as a signaling domain that binds to ligands and interacts with co-regulators (di Masi et al., 2009; Weikum et al., 2018). The structure of the LBD consists of 12 α-helices and a five-stranded antiparallel β-sheet that fold into a three-layered α-helical sandwich. This extended β-sheet is unique to PXR, as other NRs typically contain a LBD with two or three-stranded β-sheets (di Masi et al., 2009). A result of the folding pattern is the creation of the hydrophobic ligand-binding pocket (LBP) at the base of the receptor. The base of the receptor domain, including the LBP, has shown to be less conserved than the rest of the LBD, which likely contributes to PXRs

ability to recognize and bind various ligands. Furthermore, the LBD contains the activation function 2 (AF-2), which is comprised of helix 3, 4, and 12. Helix 12, or αAF, is critical for the structural organization of the AF-2 region and is highly conserved. αAF has shown to be conformationally dynamic during ligand binding, and it alters the orientation of AF-2 to ease recruitment of different co-regulators (di Masi et al., 2009; Weikum et al., 2018).

1.3.3 *Ligand binding and activation of PXR*

As mentioned previously, when a ligand binds to an NR the receptor undergoes conformational changes into an active state. However, the type of ligands able to bind to a receptor depends on several distinct structural features of the LBD. PXR exhibits several unique LBD features which might explain its ligand promiscuity: 1) the LBP of PXR is larger and more flexible than those of many other NRs (e.g., constitutive androstane receptor (CAR)); 2) the LBD comprises a flexible loop, featuring an expandable pore, which lies next to the LBP to accommodate larger sized ligands; 3) the above mentioned five-strand antiparallel β-sheet; and 4) an unique α2, which facilitates binding of large ligands in the LBP and guides entry and exit of ligands. The overall flexibility of the PXR LBP when bound by different ligands (e.g., rifampicin) is evident when compared to the apo form of the LBD (Figure 5) (Timsit & Negishi, 2007).

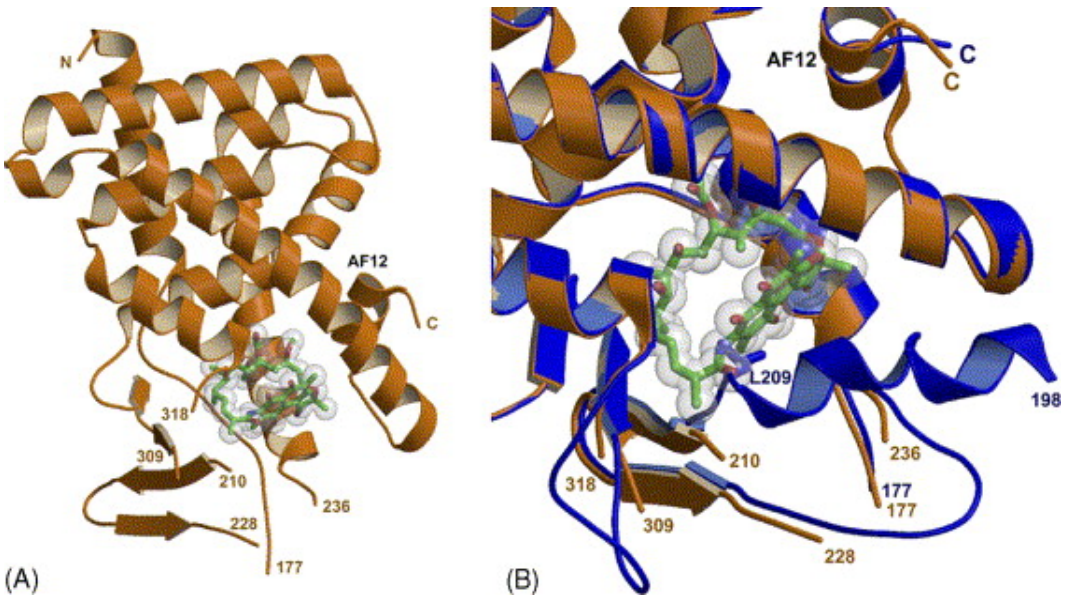

Figure 5. Comparison of human PXR-LBD bound by rifampicin to human PXR-LBD in apo form. A) Human PXR-LBD (orange) bound by rifampicin (green). B) Human PXR-LBD (orange) bound by rifampicin (green) superimposed with the unligated human PXR-LBD in non-active apo-form (blue). The crystal structures are retrieved from Timsit & Negishi (2007).

1.3.4 *Exogenous PXR ligands*

The PXR exhibits a broad ligand promiscuity compared to other NRs, which is largely due to its large and flexible LBP, in addition to structural differences such as poor conservation of the NTD (Timsit & Negishi, 2007). Furthermore, PXR ligand binding specificity has shown to be species dependent, which could be due to amino acid substitutions of ortholog protein sequences (di Masi et al., 2009; Timsit & Negishi, 2007). As the PXR exhibit an important role of the chemical defensome, as a xenosensor, several studies focusing on PXR ligand binding and activation have emerged. In general, PXR has shown the ability to bind and be activated by various xenobiotic compounds, including rifampicin, clotrimazole, and butyl 4-aminobenzoate (Chrencik et al., 2005; Creusot et al., 2021; Lille-Langøy et al., 2015; Lille-Langøy et al., 2018; Milnes et al., 2008). Rifampicin and clotrimazole have exhibited species-specific activation of PXR, and have previously been used as positive control agonists in ligand-binding assays of human PXR and zebrafish PXR, respectively (Milnes et al., 2008).

The three abovementioned xenobiotics are compounds of variable sizes and properties (Figure 6), but all are used in medical contexts. Rifampicin is a semisynthetic antibiotic with major activity against mycobacteria, in addition to having roles such as an RNA polymerase inhibitor, a DNA synthesis inhibitor, an antitubercular agent, protein synthesis inhibitor, and PXR agonist (Information, 2022c). Clotrimazole is an synthetic imidazole antifungal agent used to treat skin, oral, and vaginal candida infections, and it inhibits biosynthesis of sterols (Information, 2022b). Finally, butyl 4-aminobenzoate is a benzoate ester and is mainly used as a local anesthetic for surface anesthesia of the skin and mucous membranes (Information, 2022a).

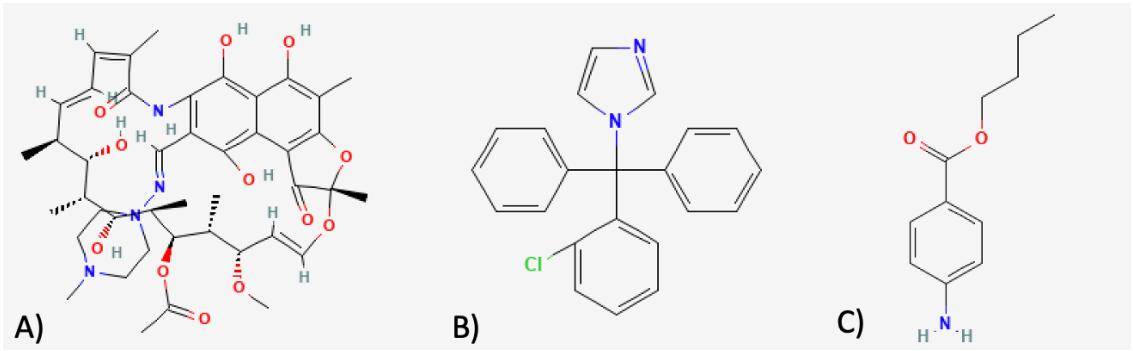

Figure 6. Exogenous ligands capable of inducing PXR activation through ligand binding. Structural illustrations of A) rifampicin, B) clotrimazole, and C) butyl 4-aminobenzoate. Structures are retrieved from PubChem (Information, 2022a, 2022b, 2022c).

1.4 *PXR in Teleosts*

The aquatic environment is a sink for man-made compounds, and teleost fishes are vulnerable to chemical stressors in their natural habitats. Exposure to such chemical stressors may have a strong impact on organism health, including viability, growth, performance, and reproductive abilities. Teleosts are also widely used as model organisms to assess potential toxic effects of chemicals, including zebrafish, medaka, Atlantic killifish, and Atlantic cod (Aranguren-Abadía et al., 2020; Blewett, Ransberry, McClelland, & Wood, 2016; Chen et al., 2011; Dai et al., 2014; Eide et al., 2021; Nacci et al., 2009; Yadetie, Karlsen, Eide, Hogstrand, & Goksøyr, 2014). As PXR is as an important xenosensor that regulates expression of several defense genes as a response to chemical stress, the presence of PXR would appear natural in teleost fishes. However, although PXR in model teleosts such as zebrafish are relatively well described (Lille-Langøy et al., 2018), little is known about the structure and functions of PXR in other teleost species. A genome mining study searching for PXR in 76 teleosts was published by Eide et al. (2018), and quite surprisingly a loss of the *pxr* gene was observed in over half of these species (Figure 7). Interestingly, the *pxr* gene was absent in most of the species belonging to the *Gadiformes* order, including Atlantic cod (*Gadus morhua*), however, it was apparently retained in the European hake (*Merluccius merluccius*). The presence of *pxr* in European hake, opposed to the absence of *pxr* in most Gadiformes, raises several interesting questions from an evolutionary and toxicological perspective, such as: is the *pxr* identified in hake a functional gene, and does it constitute the same physiological role in hake as observed in other species (e.g., teleosts and mammalians). As of today, the complete primary structure, ligand activation properties, and physiological functions (incl. target genes) of hake PXR have yet to be characterized and is pivotal for understanding the role of PXR as a NR in hake.

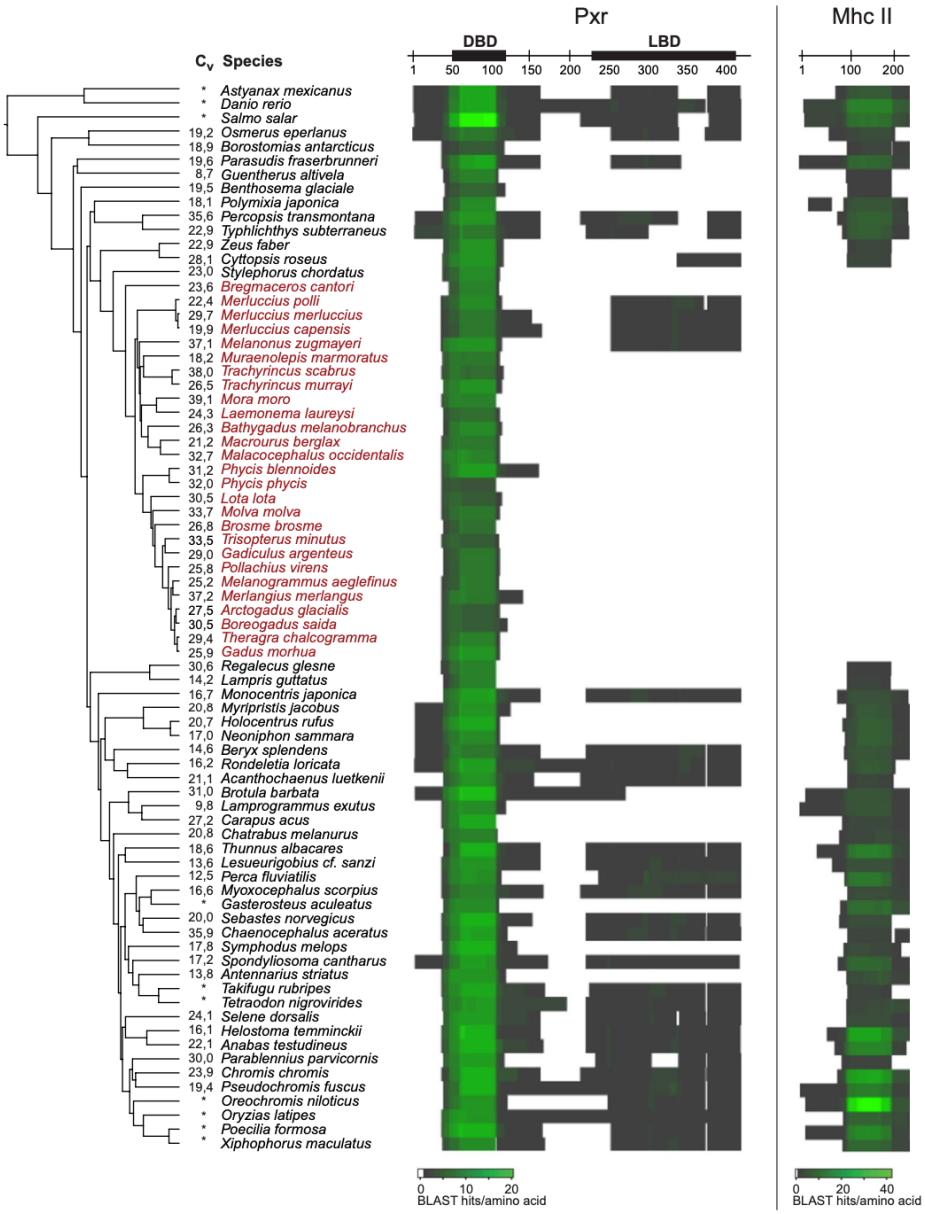

Figure 7. Identification of *pxr* in teleost fishes. *In silico* searches (using the *pxr* gene from zebrafish) of 76 teleost fish genomes for the *pxr* gene showed the loss of the *nr1i2* gene in many teleost fishes. Searches was iterated using zebrafish major histocompability class II (Mhc II) as a control. Each row represents the sequence coverage vectors of the *pxr* or *mhcii* BLAST hits in the 76 different fish species. Both DBD and LBD in zebrafish Pxr are indicated. Fish belonging to the *Gadiformes* order are highlighted in red. The figure is retrieved from Eide et. al. (2018).

1.6 *Aim of the study*

PXR has not previously been characterized on a molecular or functional level in European hake (*Merluccius merluccius*). Therefore, this study aims to uncover and characterize the primary structure and phylogeny of hake PXR, and to investigate its function as a xenosensor. *Pxr* will therefore be cloned from hake, sequenced, and integrated into a luciferase-based

reporter gene assay. This reporter gene assay will be used to functionally characterize hake PXR by investigating if three model PXR ligands, including rifampicin, clotrimazole, and butyl 4-aminobenzoate, are able to activate this receptor. As ligand binding and activation of PXR from human and zebrafish with these ligands are well characterized, PXR from these species were chosen for comparing potencies and efficacies with the same reporter gene assay. The specific objectives for this study are listed below.

i. Clone and sequence the hake *pxr* (hinge-region and LBD)
ii. Perform bioinformatical analyses of hake PXR DNA- and protein sequences, including phylogenetic analysis and annotation of functional domains and ligand binding residues.
iii. Establish an *in vitro* reporter gene assay to examine ligand-binding and activation of the hake PXR and conduct comparative studies with human- and zebrafish PXR.

2. Materials

2.1 *Chemicals and reagents*

Table 1. List of used chemicals and reagents

Name	Chemical formula	Supplier
100x protease inhibitor cocktail	-	Sigma-Aldrich
10X loading buffer	-	TaKaRA
2-Log DNA ladder	-	New England Biolabs
2-β-Mercaptoethanol	C_2H_6OS	Sigma-Aldrich
5-Carboxyfluorescein diacetate, Acetoxymethyl ester (5-CFDA-AM)	$C_{28}H_{20}O_{11}$	Thermo Fisher Scientific
Acetic acid	CH_3CO_2H	Sigma-Aldrich
Acrylamide-Bis	-	Bio-Rad
Adenosine 5´-triphosphate disodium salt trihydrate (ATP)	$C_{10}H_{20}N_5Na_2O_{16}P_3$	Sigma Aldrich
Agar-agar	-	Merck
Agarose	-	Sigma-Aldrich
Ammonium persulfate (APS)	$(NH_4)_2S_2O_8$	Sigma-Aldrich
Ampicillin sodium salt	$C_{16}H_{18}N_3NaO_4S$	Sigma-Aldrich
Bovine serum albumin (BSA)	-	Sigma-Aldrich
CHAPS	$C_{32}H_{58}N_2O_7S$	Thermo Fisher
Coenzyme A trilithium salt	$C_{21}H_{33}Li_3N_7O_{16}P_3S$	Sigma-Aldrich
Dimethyl sulfoxide (DMSO)	C_2H_6OS	Sigma-Aldrich
Disodium hydrogen phosphate	Na_2HPO_4	Sigma-Aldrich
DL-Dithiothreitol (DTT)	$HSCH_2CH(OH)CH(OH)CH_2SH$	Sigma-Aldrich
D-luciferin sodium salt	$C_{11}H_8N_2O_3S_2$	Biosynth
Dulbecco´s modified Eagle´s medium (with phenol red) (DMEM)	-	Sigma-Aldrich
Dulbecco´s modified Eagle´s medium (w/o phenol red) (DMEM)	-	Sigma Aldrich
Erythrosine B	$C_{20}H_6I_4Na_2O_5$	Sigma-Aldrich
Ethanol	CH_3CH_2OH	Sigma-Aldrich

Ethidium bromide	$C_{21}H_{20}BrN_3$	Sigma-Aldrich
Ethylene glycol-bis(β-aminoethylether) -N,N,N′,N′-tetraacetic acid (EGTA)	$C_{14}H_{24}N_2O_{10}$	Sigma Aldrich
Ethylenediaminetetraacetic acid (EDTA)	$C_{10}H_{16}N_2O_8$	Sigma Aldrich
Fetal bovine serum (FBS)	-	Sigma-Aldrich
Galactose	$C_6H_{12}O_6$	Sigma-Aldrich
Gel Red®	-	Biotium
Glycerol	$C_3H_8O_3$	Sigma-Aldrich
Isopropanol	C_3H_8O	Kemetyl
L-α-Phosphatidylcholine	-	Sigma-Aldrich
L-glutamine	$C_5H_{10}N_2O_3$	Sigma-Aldrich
Magnesium carbonate hydroxide pentahydrate	$(MgCO_3)_4•Mg(OH)_2•5H_2O$	Sigma-Aldrich
Magnesium chloride	$MgCl_2$	Sigma-Aldrich
Magnesium chloride hexahydrate	$MgCl_2•6H_2O$	Sigma-Aldrich
Magnesium sulfate	$MgSO_4$	Sigma-Aldrich
Magnesium sulfate heptahydrate	$MgSO_4•7H_2O$	Sigma-Aldrich
Methanol	CH_3OH	Sigma-Aldrich
Monosodium phosphate	NaH_2PO_4	Sigma-Aldrich
o-Nitrophenyl β-D-galactopyranoside (ONPG)	$C_{12}H_{15}NO_8$	Sigma-Aldrich
Opti-MEM® I reduced serum medium	-	Gibco
Polysorbate 20 (Tween 20)	$C_{58}H_{114}O_{26}$	Thermo Fisher
Penicillin-Streptomycin	-	Sigma-Aldrich
Phenylmethylsulfonyl fluoride (PMSF)	$C_7H_7FO_2S$	Sigma-Aldrich
Phosphate-buffered saline (PBS)	$Cl_2H_3K_2Na_3O_8P_2$	Sigma-Aldrich
Potassium chloride	KCl	Sigma-Aldrich
Potassium phosphate monobasic	KH_2PO_4	Merck
Resazurin sodium salt	$C_{12}H_6NNaO_4$	Sigma-Aldrich
Sodium chloride	NaCl	Merck
Sodium dodecyl sulfate (SDS)	$NaC_{12}H_{25}SO_4$	Merck

Sodium dihydrogen phosphate monohydrate	$NaH_2PO_4•H_2O$	Merck
Sodium Pyruvate	$C_3H_3NaO_3$	Sigma-Aldrich
TransIT®-LT1	-	Mirus Bio
Tricine	$C_6H_{13}NO_5$	Sigma-Aldrich
Tris-hydrochloric acid	HCL	Sigma-Aldrich
Trition™ X-100	-	Sigma-Aldrich
Trypsin-EDTA 1x	-	Sigma-Aldrich
Tryptone	-	Merck
Yeast extract	-	Sigma-Aldrich

2.2 *Primers*

Table 2. List of forward (fwd, f) and reverse (rev, r) primers used

ID	Name	Sequence 5′→3′
MT2087*	HaPXR_f_EcoR1	aagtccGAATTCATGTGCCAGGACATGATC
MT2089*	HaPXR_r_Nhe1	aatcgtGCTAGCTCAGGGGTCCTTCTTCAC
MT2094*	HaPXR_r_Nhe1_mut	aatcgtGCTAGCTCAGGGGTCTTTCTTCAC
MT41	T3 Fwd	ATTAACCCTCACTAAAGGGA
MT42	T7 rev	TAATACGACTCACTATAGGG
MT1077	PCMX fwd	TGCCGTCACAGATAGATTGG
MT1279	PCMX rev	AATCTCTGTAGGTAGTTTGTCCA
MT2097	HaPXR_f_midprimer	CATGATTCAGAACGTCATTG
MT2098	HaPXR_r_midprimer	AGTCTCTTGGAGAAGTCAAT
MT2066	GAL4_rev	CGATACAGTCAACTGTCTTTGAC
18418-020	$Oligo(dT)_{20}$	Invitrogen

*MT2087, MT2089 and MT2094 are the primer pairs designed for amplification and cloning of hakePXR-hinge-LBD. The six nucleotides written in small letters represents the extra nucleotides added to the 5′end of the recognition site to ensure efficient cleavage using the restriction enzyme of choice (EcoR1 and Nhe1). The six underlined nucleotides (capital letters) represent the recognition site for the restriction enzyme, while the rest of the primer sequence is complementary to each end of the hakePXR-hinge-LBD DNA sequence (fwd and rev).

2.3 *Enzymes*

Table 3. List of used enzymes

Name	Supplier
Big dye terminator v3.1	Applied Biosystems
DreamTaq green DNA polymerase	Thermo Fisher Scientific
EcoR1 – Restriction enzyme	Takara
Nhe1 – Restriction enzyme	Takara
Phusion Hot Start II DNA polymerase	Thermo Fisher Scientific
RNase H	Invitrogen
RNase OUT™ Recombinant RNase inhibitor	Invitrogen
Superscript® IV Reverse Transcriptase	Invitrogen
Shrimp alkaline phosphatase (SAP)	Affymetrix
T4 DNA ligase	Takara

2.4 *Commercial Kits*

Table 4. List of commercial kits used

Name	Application	Supplier
BigDye Terminator v3.1 cycle sequencing kit	Sanger sequencing	Thermo Scientific
DreamTaq green DNA polymerase kit	Colony PCR	Thermo Scientific
NucleoBond® PC 100 plasmid purification kit	Plasmid purification, midi	Macherey-Nagel
NucleoSpin® plasmid purification kit	Plasmid purification, mini	Macherey-Nagel
Phusion Hot Start II DNA polymerase kit	PCR amplification of hakePXR from cDNA	Thermo Scientific
StrataClone Blunt PCR cloning kit	Blunt cloning into pSC-B	Agilent
Superscript® IV Reverse Transcriptase kit	cDNA synthesis	Invitrogen
T4 DNA-ligase kit	Ligate hakePxr and pCMX	Takara
SuperSignal™ West Pico PLUS Chemiluminescent Substrate kit	Protein expression verification in COS-7 cells	Thermo Scientific
Zymoclean™ Gel DNA Recovery Kit	DNA purification	ZYMO Research

2.5 *Cell lines*

Table 5. List of cell lines used throughout the thesis

Name	Description	Supplier
COS-7 cells	African green monkey kidney cells (eukaryote)	-
StrataClone SoloPack Competent Cells	*Escherichia coli* (prokaryote)	Agilent
StrataClone "Mix&GO" Competent Cells	*Escherichia coli* (prokaryote)	Agilent

2.6 *Plasmids*

Table 6. List of the different plasmids used

Name	Application
(MH100)x4 tk luc	LRA, reporter plasmid
pCMV-β-Gal	LRA, control plasmid
pCMX-GAL4-DBD	Construction of pCMX-GAL4-HakePXR
pCMX-GAL4-hakePXR	LRA, receptor plasmid
pCMX-GAL4-humanPXR	LRA, receptor plasmid
pCMX-GAL4-zebrafishPXR-TL	LRA, receptor plasmid
pSC-B	Blunt end cloning vector
pSC-B-hakePXR	Construction of pCMX-GAL4-HakePXR

2.7 *Cell growth mediums*

Table 7. Lysogeny Broth (LB) medium

Components	LB-medium (conc.)	LB-agar plates (conc.)
Agar-agar	-	15 g/L
Ampicillin*	-	100 mg/L
MQH_2O	-	-
NaCl	10 g/L	10 g/L
Tryptone	10 g/L	10 g/L
Yeast Extract	5 g/L	5 g/L

*Added post autoclavation

Table 8. Cultivation and freezing medium for COS-7 cells

Components	Cultivation medium (conc.)	Cultivation medium, exposure (conc.)	Freezing medium (conc.)
DMEM with phenol red	1 X	-	1 X
DMEM w/o phenol red	-	1 X	-
FBS	10%	-	10%
FBS charcoal stripped	-	10%	-
L-glutamine	4 mM	4 mM	4 mM
Sodium pyruvate	1 mM	1 mM	1 mM
Penicillin-Streptomycin	100 U/mL, 0.1 mg/mL	100 U/mL, 0.1 mg/mL	100 U/mL, 0.1 mg/mL
DMSO	-	-	5%

2.8 *Buffers and solutions*

2.8.1 *Agarose gel electrophoresis*

Table 9. TAE buffer (1X)

Component	Concentration
Tris	40 mM
Acetic acid	20 mM
EDTA	1 mM

Table 10. Agarose gel

Component	Concentration
Agarose	0.7 - 1 %
GelRed 10000x	0.0014%
TAE-buffer	1X

2.8.2 *Western blot assay*

Table 11. Running and stacking gel for one 12% SDS-page

Components	12% Running Gel	Stacking Gel
ddH_2O	2.49 mL	2.27 mL
30% Acrylamide-Bis	3.0 mL	0.65 mL
1.5 M Tris pH 8.8	1.9 mL	-
0.5 M Tris pH 6.8	-	1.0 mL
20% SDS	37.5 µL	20.0 µL
10% APS	75.0 µL	40.0 µL
TEMED	3.0 µL	4.0 µL

Table 12. 5X Sample buffer

Component	Concentration
Tris HCl pH 6.8	250 mM
SDS	10%
Glycerol	30%
2-β-mercaptoethanol	5%
Bromophenolblue	0.02%

Table 13. Lysis buffer for sample preparation

Component	Concentration
5X Sample buffer	2X
10X PBS pH 7.4	1X
100X Protease	1X
inhibitor	-
ddH_2O	

Table 14. 10X Tris-buffered saline (TBS) pH 7.5

Component	Concentration
Tris base	24 g
NaCl	88 g
MQH_2O	900 mL
32-N-HCL	pH adjustment

Table 15. 1X TGS running buffer

Component	Concentration
Glycine	192 mM
Tris base	25 mM
SDS	0.1%

Table 16. 10X Tris-glycine (TG) buffer

Component	Concentration
Glycine	14.4 g
Tris base	30.3 g
MQH_2O	-

Table 17. 0.1% TBS-Tween (TBST)

Component	Concentration
10X TBS	0.5 X
Tween 20	0.1%
MQH_2O	-

Table 18. 1X Transfer buffer (TG)

Component	Concentration
10X TG buffer	100 mL
Methanol	200 mL
MQH_2O	700 mL

Table 19. Blocking solution (7% milk)

Component	Concentration
Powder milk	3.5 g
TBS-Tween	50 mL

2.8.3 *Luciferase reporter gene assay*

Table 20. Cell lysis base buffer (1X, pH 7.8)

Component	Concentration
TrisHCl pH 7.8	25 mM
Glycerol	15%
CHAPS	2%
L-α-Phosphatidylcholine	1%
BSA	1%

Table 21. Cell lysis reagent solution

Component	Concentration
Cell lysis base buffer	1X
EGTA	4 mM
DTT	1 mM
$MgCl_2$	8 mM
PMSF	0.4 mM

Table 22. β-galactosidase base buffer (10X, pH 7.2)

Component	Concentration
Na_2HPO_4	60 mM
$NaH_2PO_4•H_2O$	40 mM
KCl	10 mM
$MgCl_2•6H_2O$	1 mM

Table 23. β-galactosidase reagent solution

Component	Concentration
β-gal base buffer	1X
DTT	5.5 mM
ONPG	8.6 mM

Table 24. Luciferase base buffer (4X, pH 7.8)

Component	Concentration
Tricine	80 mM
$(MgCO_3)_4•Mg(OH)_2•5H_2O$	4.28 mM
Na_2EDTA	0.4 mM
$MgSO_4•7H_2O$	10.68 mM

Table 25. Luciferase reagent solution

Component	Concentration
Luciferase base buffer	1X
MQH_2O	-
DTT	5 mM
ATP	0.5 mM
Coenzyme A*	0.2 mM
D-luciferin*	0.5 mM

*Added just before use

2.8.4 *Cell viability assay*

Table 26. L-15/ex solution A

Component	Concentration
NaCl	80.0 g
KCl	4.0 g
$MgSO_4•7H_2O$	2.0 g
$MgCl_2•6H_2O$	2.0 g
MQH_2O	600 mL

Table 27. L-15/ex solution B

Component	Concentration
$CaCl_2$	1.4 g
MQH_2O	100 mL

Table 28. L-15/ex solution C

Component	Concentration
Na_2HPO_4	1.9 g
KH_2PO_4	0.6 g
MQH_2O	300 mL

Table 29. L-15/ex cell viability solution

Component	Concentration
ddH_2O	500 mL
L-15/ex solution A	34 mL
L-15/ex solution B	6 mL
L-15/ex solution C	17 mL
Galactose	0.8 mg/mL
Pyruvate	0.5 mg/mL
Resazurin	0.03 mg/mL
CFDA-AM	0.001 mg/mL

2.9 *Antibodies*

Table 30. Primary and secondary antibodies used

Name	Supplier
Anti-GAL4[DBD] Antibody (RK5C1):SC-510 mouse monoclonal IgG2a	Santa Cruz
ECL Anti-mouse IgG HRP linked whole antibody (from sheep), polyclonal, NA931V	GE healthcare
Anti-β-actin mouse monoclonal antibody, Ab8224	Abcam

2.10 *Ligands used for luciferase reporter gene assay and cell viability assay*

Table 31. Ligands used for LRA and cell viability

Name	Catalog number	Supplier
Clotrimazole	C6019	Sigma-Aldrich
Rifampicin	R3501	Sigma-Aldrich
Butyl 4-aminobenzoate	06970	Sigma-Aldrich

2.11 *Instruments*

Table 32. List of instruments used

Name	Application	Supplier
Burker hemocytometer	Cell counting (COS-7 cells)	Marienfield
ChemiDoc™ XRS+ system	Agarose gel picture	
CleanAir EuroFlow Class II biosafety cabinet	Workspace for sterile handling of COS-7 cells	Baker
DM IL inverted microscope	Cell count, visualize confluency	Leica
GD100	Heat-shock cells, water bath	Grant
Heraeus Pico 21	Centrifuge	Thermo Scientific
Heraeus multifuge X3R	Centrifuge	Thermo Scientific
Hidex Sense Microplate Reader	Plate reader	Hidex
HS 501 Digital	Plate shaker	IKA®-Werle
MilliQ A10 advantage	MQH_2O dispenser	Merck
MP220	pH-meter	Bergman

Multitron Standard Shaking incubator	Cell cultivation	Infors HT
Nanodrop 1000	Measure RNA, DNA and cDNA concentrations	Thermo Scientific
Panasonic mco-170aicuv-pe	Incubation of COS-7 cells	Lab-Tec
PowerPac™ HC	Power supply for electrophoresis	Bio-Rad
T100™ Thermal Cycler	PCR amplification	Bio-Rad
Termaks incubator	Incubation of transformed colonies	Termaks
Thermomixer compact	Heat-block	Eppendorf
Ultraspec 10 cell density meter	Measure cell culture density	Amersham Biosciences
UV-transiluminator	Agarose gel DNA extraction	UVP

2.12 *Computer software*

Table 33. List of software and online tools used

Name	Application	Supplier
BioRender 2022	Figure preparation	BioRender®
Clustal Omega	Multiple sequence alignment	EMBL-EBI
Ensembl	Genome browser	EMBL-EBI
Excel v.16.60 2022	Data processing and statistics	Microsoft®
GraphPad Prism v.9.3.1	Figures and statistics	GraphPad Software
Jalview 2.11.2.2	Multiple sequence alignment, visualization	Waterhouse et al., 2009
MegaX v.10.2.6	Phylogenetic analysis	Stecher et al., 2020
Multiple Primer Analyzer	Secondary structure prediction	Thermo Fisher Scientific
Muscle	Multiple sequence alignment	EMBL-EBI
PowerPoint v.16.60 2022	Processing figures	Microsoft®
SnapGene® 6.0.2	Primer design, cloning simulations, sequence alignment	Dotmatics
UniProt	Genome browser	EMBL-EBI and PIR
Word v.16.60 2022	Thesis writing	Microsoft®

3. Methods

3.1 *Experimental outline*

Throughout this thesis several molecular biology methods have been utilized in the laboratory, in addition to bioinformatical analyses. Figure 8 shows the experimental outline, highlighting the most significant methods used.

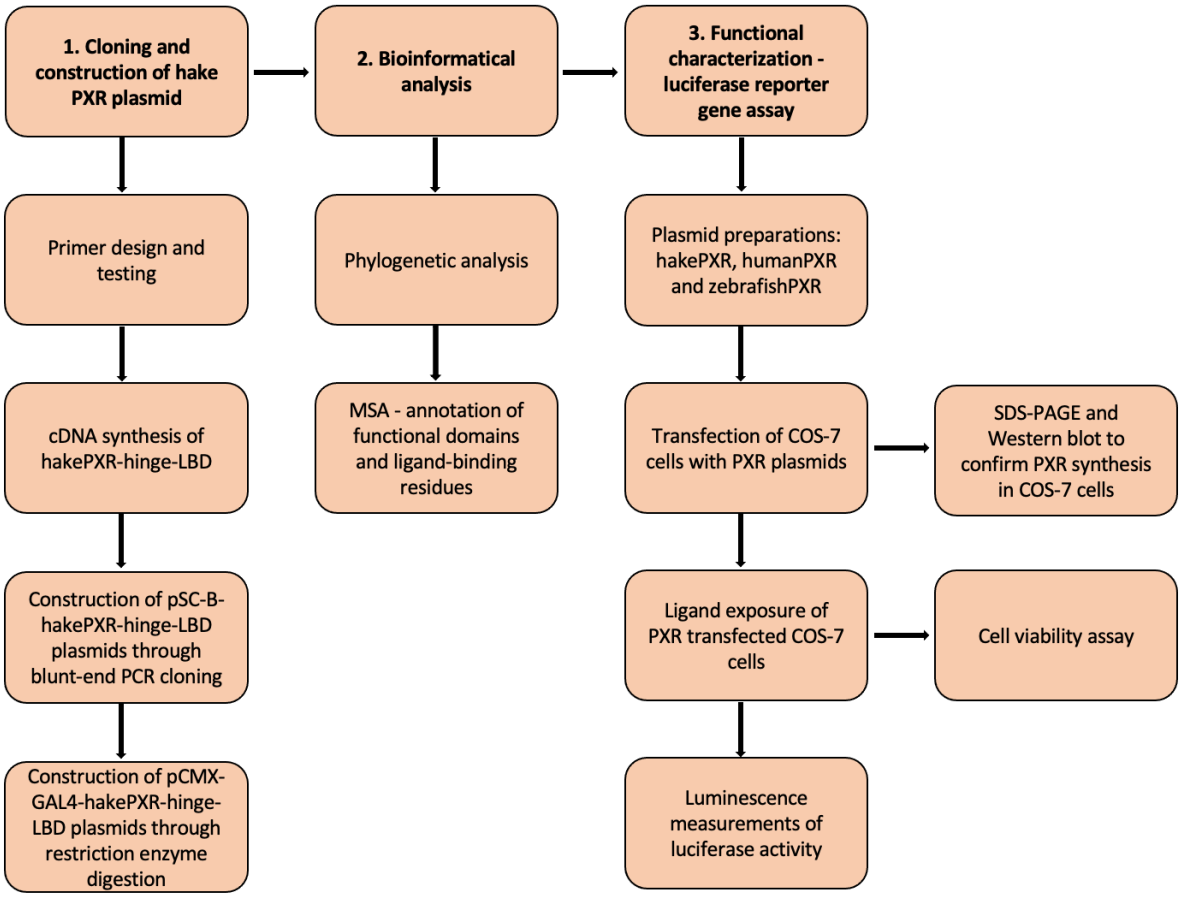

Figure 8. Experimental outline. Hake (*Merluccius merluccius*) cDNA was prepared from an RNA sample retrieved from liver tissue. The hake PXR hinge-LBD region was cloned from cDNA and inserted into a pSC-B vector through blunt-end PCR cloning. Thereafter, pCMX-GAL4-hakePXR-hinge-LBD expression plasmids were constructed through restriction enzyme digestion and ligation. Sanger sequencing was used to verify the correct incorporation of hakePXR into the plasmid. Bioinformatical analyses were applied to investigate PXR amino acid sequence similarities across different species, and a phylogenetic three and a MSA of hake, human (*Homo sapiens*) and zebrafish (*Danio rerio*) PXR was created. hakePXR, humanPXR and zebrafishPXR expression plasmids were isolated and used to transfect COS-7 cells. SDS-PAGE and Western blot were further used to verify synthesis of the PXR fusion proteins in transfected COS-7 cells. After ligand exposure, activation of PXR was measured in luciferase reporter gene assays, while cytotoxicity of test compounds was monitored through a cell viability assay.

3.2. *Complementary DNA synthesis*

Complementary DNA (cDNA) was synthesized using a reverse transcriptase and RNA as template. The RNA sample was retrieved from hake liver tissue and was obtained from the preexisting RNA tissue bank in our laboratory. Superscript® IV Reverse Transcriptase was used for the cDNA synthesis reaction, and its protocol was followed accordingly. The kit includes two different primers; Oligo(dT)$_{20}$ primer and random hexamers, out of which the Oligo(dT)$_{20}$ primer was used. Oligo(dT)$_{20}$ primer consist of strings of 20 deoxythymidylic acid residues that can bind and hybridize to the poly(A) tale of mRNA. First, the components constituting the RNA-primer mix (Table 34) was combined and incubated at 65℃ for 5 min and then left on ice. The RT reaction mix (Table 35) was then prepared and added to the RNA-primer mix. The mix was briefly centrifuged, and the polymerase chain reaction (PCR) program was run (Table 36) using a T100™ Thermal Cycler. Synthesized cDNA was treated with RNase H to remove RNA, before concentration and purity was determined with a Nanodrop 1000 and stored at -20℃.

Table 34. RNA-primer mix for cDNA synthesis

Components	Volume	Concentration
Oligo(dT)$_{20}$	1.0 µL	2.5 µM
dNTP mix	4.0 µL	0.5 mM
Template RNA	4.9 µL	2 µg
Nuclease free H_2O	3.1 µL	-

Table 35. RT reaction mix for cDNA synthesis

Components	Volume	Concentration
5x SSIV Buffer	4.0 µL	1X
DTT	1.0 µL	5 mM
RNaseOUT Recombinant RNase inhibitor	1.0 µL	2 U/µL
Superscript IV Reverse Transcriptase	1.0 µL	10 U/µL

Table 36. PCR program for cDNA synthesis

Temperature	Time	Cycles
50℃	10 min	
80 ℃	10 min	1

3.2.1 *Polymerase chain reaction*

Polymerase chain reaction (PCR) is a method that is used to amplify specific, or unspecific, DNA sequences by using primers (single-stranded oligos). The process usually involves preparation of a master mix, which includes buffer, dNTPs, primers, polymerase, and template DNA, before the PCR program is performed. The PCR program normally consists of a three-step cycle which is repeated until the preferred amount of DNA is produced, generally 20-40 cycles. Denaturation is the first step, where double-stranded DNA normally is heated to around 95℃ to break it into two single strands of DNA. The next step is annealing, where the temperature is lowered enough for the primers to attach to the single-stranded DNA template. Elongation is the last step, where the sample is heated to the optimal temperature for DNA-polymerase activity, which normally is 72℃. The DNA-polymerase synthesize new second strands to the DNA, doubling the amount of double-stranded DNA. As this three-step cycle is repeated the amount of DNA increases exponentially.

3.3 *Construction of pSC-B-hakePXR plasmid by blunt-end PCR cloning*

3.3.1 *Primer design and PCR amplification of PXR sequence from cDNA*

Specific primer pairs, forward (5') and reverse (3′), were designed for amplification of the hakePXR-hinge-LBD DNA sequence from synthesized cDNA. The amplified DNA fragment was subsequently used for construction of the pSC-B-hakePXR-hinge-LBD and the pCMX-GAL4-hakePXR-hinge-LBD plasmids (Methods 3.3 – 3.4). The forward primer and the reverse primer were designed to bind at the N-terminal side of the hinge-region and to the far C-terminal of the LBD, respectively.

To ensure optimal and specific binding to cDNA, the primers were 20-30 nucleotides in length, had a GC content of 40-60%, and a melting temperature (T_m) that differed by less than 5℃ between the primer pairs. In addition, recognition sites for specific restriction enzymes were incorporated in the primers, where the forward and reverse primer included a recognition site for EcoR1 and Nhe1, respectively. Restriction enzymes are endonucleases that bind and cut specific DNA sequences, which were used to construct the pCMX-GAL4-hakePXR-hinge-LBD plasmids.

SnapGene 6.0.2 was used to design the primers and perform an *in-silico* cloning simulation. Thermo Fisher Scientific Multiple Primer Analyzer was used for secondary structure prediction and to check for formation of primer dimers. Primers were tested and used to amplify the hakePXR-hinge-LBD sequence through PCR amplification. The PCR products were visualized with agarose gel electrophoresis on a 1% agarose gel (Method 3.3.2).

Table 37. Primers designed and used for PCR amplification of hakePXR-hinge-LBD sequence

ID	Name	Sequence 5′→3′
MT2087	HaPXR_f_EcoR1	aagtccGAATTCATGTGCCAGGACATGATC
MT2089	HaPXR_r_Nhe1	aatcgtGCTAGCTCAGGGGTCCTTCTTCAC
MT2094	HaPXR_r_Nhe1_mut	aatcgtGCTAGCTCAGGGGTCTTTCTTCAC

Table 38. Reagents for PCR amplification of hakePXR-hinge-LBD

Components	Volume	Concentration
5x Phusion HF buffer	10.0 µL	1x
dNTPs	1.0 µL	200 µM
Fwd primer	2.5 µL	0.5 µM
Rev primer	2.5 µL	0.5 µM
Template	5.0 µL	-
Phusion hotstart polymerase	0.5 µL	1 U
MQH_2O	To 50 µL	-

Table 39. PCR program for amplification of hakePXR-hinge-LBD

Temperature	Time	Cycles
98°C	30 sec	-
98°C 60°C 72°C	10 sec 30 sec 38 sec	40
72 °C	5 min	-
4°C	∞	-

3.3.2 *Agarose gel electrophoresis*

Agarose gel electrophoresis was used to separate, visualize, and analyze DNA samples, including PCR products and plasmid samples. Agarose electrophoresis is used to separate DNA by size-dependent migration through an electric field. As DNA is negatively charged it will migrate towards the positive electrode (anode), where the smaller fragments are able to migrate longer distances through the porous gel.

Agarose and 1x TAE buffer was mixed and heated to produce the desired percentage agarose gel, between 0.7-1%. 0.5 µL GelRed was added to the agarose gel (30 mL or 50 mL), before the gel was left to solidify. GelRed is a fluorescent nucleic acid stain which makes it possible to visualize the DNA samples. After the gel had set, it was submerged with 1x TAE. The DNA samples were mixed with 10X loading buffer (which make the samples descend to the bottom of the wells) before being loaded into wells on the agarose gel. A 2-log DNA ladder was used to indicate the size of the separated DNA fragments. The gel was run at 80V for 1 hour, and then visualized with the ChemiDoc™ XRS+ system (Bio-Rad).

3.3.3 *Gel DNA recovery*

After agarose gel electrophoresis, DNA was recovered and purified from the gel by using Zymoclean™ Gel DNA Recovery kit (ZYMO Research). The gel was first placed on a UV-table to visualize the DNA bands, then the band of interest was excised with a scalpel and transferred to an Eppendorf tube. Agarose Dissolving Buffer (ADB) was added to the gel, and then incubated at 45℃ until the gel was dissolved. The melted agarose solution was transferred to a Zymo-Spin™ Column in a collection tube where DNA was bound to the membrane, washed, and centrifuged. DNA was eluted using a Tris-HCl DNA elution buffer (pH 8.5). Concentration of the recovered DNA was measured with the Nanodrop 1000 instrument. Purified PCR products were stored at -20℃.

3.3.4 *Blunt-end PCR cloning and transformation of Escherichia coli*

StrataClone Blunt PCR cloning kit (Agilent) was used to blunt-clone purified hakePXR-hinge-LBD fragments (PCR products) into pSC-B-vectors, creating the pSC-B-hakePXR-hinge-LBD plasmids (Figure 9). The constructed plasmids were then transformed into StrataClone Solopack Competent Cells, which are competent *Escherichia coli* (*E. coli*) cells.

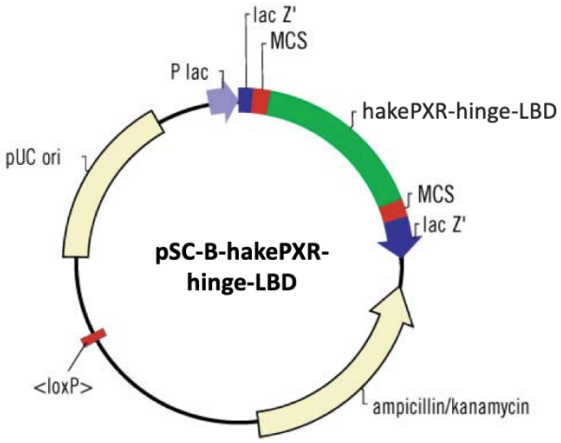

Figure 9. pSC-B-hakePXR-hinge-LBD plasmid. The plasmid constructed by blunt-end PCR cloning is visualized, including the pSC-B vectors different features and the multiple cloning site (MCS) where the hakePXR-hinge-LBD DNA fragment (PCR product) is ligated into. The illustration is adapted from the Agilent StrataClone Blunt PCR Cloning kit instruction manual.

A ligation reaction mixture was prepared by combining 3 µL StrataClone Blunt Cloning Buffer, 2 µL purified PCR product and 1 µL StrataClone Blunt Vector Mix amp/kan. The ligation mixture was incubated at room temperature (RT) for 5 min, and then placed on ice. Competent *E. coli* cells, stored at -80°C, were thawed on ice before 1 µL of the ligation mixture was added to the cells. The transformation mixture was then incubated on ice for 20 min to promote DNA binding to the cells. After incubation, the transformation mixture was heat-shocked at 42°C for 45 sec using a water bath, then quickly put on ice, and incubated for 2 min. Heat-shocking of the cells causes their membrane fluidity to change and allows the bound DNA to be absorbed into the cells. LB-medium was pre-warmed to 42°C in the water bath, then 250 µL of the medium was added to the transformation mixture. The competent cells were incubated at 37°C and 250 rpm for 1.5 hour in the Multitron Standard Shaking incubator to recover from the heat-shock. LB-agar-ampicillin plates were prewarmed to 37°C and 40 µL of 2% X-gal was spread out on each plate. Duplicates of each transformation mixture were plated for blue-white colony screening, one with 5 µL mix + 100 µL LB-medium and one with 100 µL mix. The plates were incubated overnight at 37°C.

3.3.5 *Blue-White colony screening*

The pSC-B vector used to transform the competent *E. coli* cells contained a gene that coded for ampicillin resistance, and thereby only cells that had successfully taken up the plasmid would grow on the LB-agar-ampicillin plates. Blue-white screening of the bacteria colonies was performed to further differentiate between colonies containing recombinant plasmid (containing PCR insert) and non-recombinant plasmid (no insert).

Both the vector and the *E. coli* cells used contain a segment of the lacZ gene, which can associate to form a functional protein (β-galactosidase). This complementation is called α-complementation. The multiple cloning site (MCS) is embedded in the lacZ-α gene in the vector but does not disturb the reading frame. Therefore, cells with non-recombinant plasmid will produce the functional β-galactosidase that metabolizes X-gal and produce a blue product. Recombinant plasmids have the PCR product inserted in the MCS which disturbs the α-complementation, meaning that no functional β-galactosidase will be synthesized. Therefore, bacterial colonies containing recombinant plasmid will have a white appearance instead of blue. Six white bacteria colonies from each of the diluted plates were chosen to proceed with.

3.3.6 *Colony PCR*

The transformed bacteria colonies were examined by colony PCR to verify the incorporation of the constructed pSC-B-hakePXR-hinge-LBD plasmid. A portion of the construct was amplified using PCR with T3 and T7 as forward and reverse primers, respectively. First, the colonies of interest were poked with a pipet tip and resuspended in 10 µL MQH_2O. Then, master mixes with the colony/MQH_2O samples as templates were prepared, and amplification was done with PCR. Agarose gel electrophoresis in a 1% agarose gel was carried out to confirm the presence of the inserted hakePXR-hinge-LBD sequence in the pSC-B plasmid.

Table 40. Primers used for colony PCR of pSC-B-hakePXR-hinge-LBD plasmids

ID	Name	Sequence 5′→3′
MT41	T3 Fwd	ATTAACCCTCACTAAAGGGA
MT42	T7 Rev	TAATACGACTCACTATAGGG

Table 41. Reagents for colony PCR

Components	Volume	Concentration
10x dream Taq green buffer	1.0 µL	1x
dNTPs	0.2 µL	200 µM
Fwd primer	0.2 µL	0.2 µM
Rev primer	0.2 µL	0.2 µM
Template	0.5 µL	-
Dream Taq polymerase	0.05 µL	0.25 U
MQH_2O	To 10 µL	-

Table 42. Colony PCR program

Temperature	Time	Cycles
95°C	3 min	-
95°C 45°C 72°C	30 sec 30 sec 1 min	30
72 °C	5 min	-
4°C	∞	-

3.3.7 *Plasmid purification - miniprep*

Miniprep was used to purify the constructed pSC-B-hakePXR-hinge-LBD plasmid-DNA, and subsequently for purification of the constructed pCMX-GAL4-hakePXR-hinge-LBD plasmids. Miniprep is a low-scale purification method with a typical yield between 25 – 45 µg DNA per sample. The NucleoSpin® plasmid purification kit (Machery-Nagel) was used for the plasmid purification, and its protocol followed accordingly.

Bacteria colonies containing the plasmid construct were cultivated in 6 mL LB-medium with ampicillin (0.1 mg/mL) overnight in the Multitron Standard Shaking incubator (Infors HT) at 37°C and 250 rpm. 500 µL of each sample was mixed with 500 µL of 50% glycerol and were stored as glycerol stocks at -80°C. The volume left in each of the *E. coli* LB culture samples was purified by miniprep. The bacteria culture was centrifuged to form a pellet, then added a resuspension buffer. The cells were further lysed with an SDS/alkaline lysis buffer to release

plasmid DNA, and then added a neutralization buffer. Cellular content such as protein, genomic DNA, and cell debris was removed by centrifugation, while the supernatant containing plasmid DNA was loaded onto a silica-based membrane and DNA was bound. A washing step with an ethanol-based buffer was performed to remove contaminants from the membrane. Finally, purified plasmid DNA was eluted in 50 µL of the slightly alkaline Buffer AE (5 mM Tris/HCl, pH 8.5). Concentration of the purified plasmid DNA was measured with Nanodrop 1000, before the sample was stored at -20℃.

3.4 *Construction of pCMX-GAL4-hakePXR*

3.4.1 *Restriction enzyme digestion*

To enable incorporation of the hakePXR-hinge-LBD sequence into the pCMX-GAL4-DBD vector, both the pSC-B-hakePXR-hinge-LBD plasmid and a pCMX-GAL4 plasmid were digested using two restriction enzymes. EcoR1 and Nhe1 were used as restriction enzymes as their recognition sequences were preexisting in the pCMX-GAL4 plasmid and earlier introduced to the hakePXR-hinge-LBD sequence through the primers used for DNA amplification.

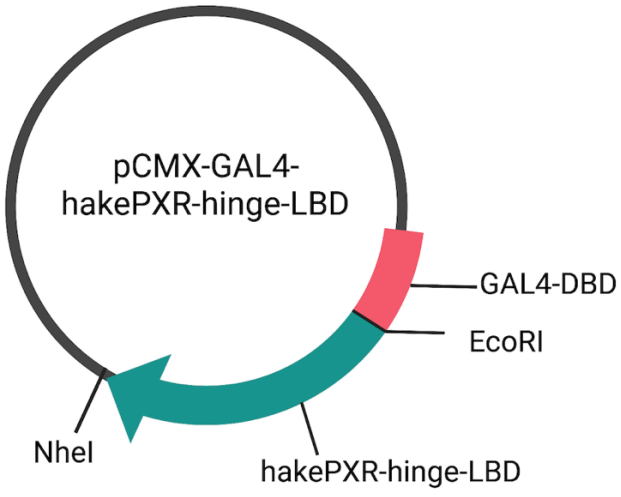

Figure 10. pCMX-GAL4-hakePXR-hinge-LBD plasmid. The plasmid constructed by restriction enzyme digestion and ligation is visualized by a simplified illustration. Restriction enzyme recognition sites used in the digestion reactions are highlighted. The illustration is created with biorender.com.

Two separate digestion reactions were set up, one for the pSC-B-hakePXR plasmid (insert) and one for the pCMX-GAL4 plasmid (vector). The digestion reactions were made according to Table 43, where the insert reaction had a total volume of 20 µL and used 1 µg template, whereas the vector reaction had a total volume of 40 µL and used 2 µg template. Both digestion reactions were incubated at 37℃ for 1.5 hour. After incubation, the insert reaction was stored at 4℃, while the vector reaction was added 1 µL Shrimp Alkaline Phosphatase (SAP) and incubated at 37℃ for 30 min. SAP was used to dephosphorylate the phosphorylated ends of DNA created during the digestion to prevent religation of the linearized pCMX-GAL4 plasmid DNA. The vector reaction was then incubated at 65℃ for 15 min to inactivate the phosphatase. Agarose gel electrophoresis on a 1% agarose gel was used to separate and visualize the digestion products. The bands corresponding to hakePXR-hinge-LBD and pCMX-GAL4-DBD were located and cut out by using a UV-table. Purified DNA was recovered from the gel bands by using Zymoclean™ Gel DNA Recovery kit (ZYMO Research) (Method 3.3.3). Concentration of the recovered DNA samples was measured with Nanodrop 1000.

Table 43. Reagents for digestion with restriction enzymes

Components	Volume	Concentration
EcoR1	1.0 µL	0.75 U/µL
Nhe1	1.0 µL	0.50 U/µL
Template (pSC-B-hakePXR or pCMX)	-	1µg or 2 µg
10X M Buffer	2 µl	1X
MQH_2O	To 20 µL	-
SAP	1 µL	1 U

3.4.2 *Ligation of hakePXR and pCMX-GAL4*

After the restriction enzyme digestions, the hakePXR-hinge-LBD and pCMX-GAL4-DBD DNA products recovered from the gel were ligated to construct the pCMX-GAL4-hakePXR-hinge-LBD plasmid. T4 DNA ligase was used for the ligation reaction, which is an enzyme that catalyzes the formation of phosphodiester bonds between phosphate and hydroxyl groups in DNA. A ligation reaction mix was prepared according to Table 44, then incubated overnight at 4℃. A 3:1 molar ratio of insert (hakePXR-hinge-LBD) and vector (pCMX-GAL4) was used.

Table 44. Reagents for ligation reaction of pCMX-GAL4 and hakePXR-hinge-LBD

Components	Volume	Concentration
Vector	-	50 ng
Insert	-	33 ng
10X T4 DNA ligase buffer	1.0 µL	1X
T4 ligase	1.0 µL	35 U/µL
MQH_2O	To 10 µL	-

3.4.3 *Transformation of Escherichia coli with ligation product*

StrataClone "Mix&GO" Competent Cells were used to transform the constructed pCMX-GAL4-hakePXR-hinge-LBD plasmid into *E. coli* cells. The *E. coli* cells were stored at -80℃ and thawed on ice before use. 2.5 µL of ligation product was added to 50 µL cells and mixed gently. 150 µL LB medium was then added to the cell mix. 2 µL cell mix and 50 µL LB medium was added to one plate, and 100 µL cell mix was added to another plate. The content on the plates was evenly distributed with a sterilized glass rod, then incubated upside down overnight at 37℃. To verify the incorporator of the pCMX-GAL4-hakePXR-hinge-LBD plasmid in the transformed bacteria colonies, colony PCR and agarose gel electrophoresis were performed in accordance with method 3.3.6 but with different primers (MT1077 and MT1279). Then, glycerol stocks were made, and plasmid-DNA was purified using miniprep (method 3.3.7).

Table 45. Primers used for colony PCR of pCMX-GAL4-hakePXR-hinge-LBD plasmids

ID	Name	Sequence 5′→3′
MT1077	PCMX fwd	TGCCGTCACAGATAGATTGG
MT1279	PCMX rev	AATCTCTGTAGGTAGTTTGTCCA

3.4.4 *Sanger sequencing*

Sequencing of the pCMX-GAL4-hakePXR-hinge-LBD plasmid constructs was performed to verify the incorporation of hakePXR-hinge-LBD into the pCMX-GAL4 vector and to further examine the cloned hakePXR sequence. BigDye v3.1 was used to prepare the sequencing reaction, and its protocol was followed accordingly. First, the components constituting the sequencing reaction (Table 47) was combined where the constructed pCMX plasmids were used as template. Then, a PCR program (Table 48) was ran using T100™ Thermal Cycler. After the PCR reaction was completed, 10 µL MQH_2O was added to the reaction product and sent for sequencing at the Department of Biological Science (UiB). As sanger sequencing is limited to 900 bp, so several primers had to be utilized to allow sequencing of the whole hakePXR insert. Sequencing data was analyzed with SnapGene® 6.0.2, where sequencing results were aligned with the predicted hakePXR sequence obtained by a member of this research group through genome analysis (Eide et al., 2018).

Table 46. Primers used for sanger sequencing of pCMX-GAL4-hakePXR-hinge-LBD plasmid

ID	Name	Anneal temp.	Sequence 5′→3′
MT1077	PCMX fwd	52°C	TGCCGTCACAGATAGATTGG
MT1279	PCMX rev	52°C	AATCTCTGTAGGTAGTTTGTCCA
MT2066	GAL4_rev	52°C	CGATACAGTCAACTGTCTTTGAC
MT2097	HaPXR_f_midprimer	47°C	CATGATTCAGAACGTCATTG
MT2098	HaPXR_r_midprimer	47°C	AGTCTCTTGGAGAAGTCAAT

Table 47. Reagents used for sanger sequencing reaction

Components	Volume	Concentration
5X sequencing buffer	1.0 µL	0.5 X
Big Dye	1.0 µL	1 U
Fwd primer (3.2 µM)	1.0 µL	0.32 µM
Rev primer (3.2 µM)	1.0 µL	0.32 µM
Template	-	152.5 ng
MQH_2O	To 10 µL	-

Table 48. PCR program performed before sanger sequencing

Temperature	Time	Cycles
96°C	5 min	-
96°C 47°C / 52°C 60°C	10 sec 5 sec 4 min	25
4°C	∞	-

3.4.5 *Plasmid purification – midiprep*

Midiprep was used to purify the constructed pCMX-GAL4-hakePXR-hinge-LBD plasmid, and the remaining plasmids used in the luciferase reporter gene assay; humanPXR, zebrafishPXR, luciferase reporter plasmid and β-galactosidase normalization plasmid. Midiprep is a medium-scale purification method with a typical yield between 20 – 100 µg DNA per sample. The NucleoBond® PC 100 plasmid purification kit (Machery-Nagel) was used for the midiprep plasmid purification, and its protocol followed accordingly.

Bacteria cells containing the desired plasmids, retrieved from glycerol stocks, were cultivated in 200 mL LB-medium with ampicillin (0.1 mg/mL) overnight in the Multitron Standard Shaking incubator (Infors HT) at 37°C and 250 rpm. Cell density was measured at 600 nm by using Ultraspec 10 Cell Density meter (Amersham Bioscience) and optical density volume (ODV) = 200 was calculated. Plasmids were then purified by midiprep, which is similar to miniprep (Method 3.3.7), expect plasmid DNA is eluted in 5 mL elution buffer which undergoes an additional cleaning step; DNA is precipitated using isopropanol, centrifuged, washed with ethanol, and dried. Finally, purified plasmid DNA was dissolved in 150 µL of the slightly alkaline Buffer AE (5 mM Tris/HCl, pH 8.5). Concentration of the purified plasmid DNA was measured with Nanodrop 1000. Then, agarose gel electrophoresis was used to examine the plasmid conformation of all purified plasmids by loading 200 ng of each sample on a 1% agarose gel. Purified plasmid samples were stored at -20°C.

3.5 *Bioinformatical analyses*

3.5.1 *Phylogenetic analysis*

A phylogenetic tree was produced to visualize the evolutionary relationship of the hake PXR with PXRs present in other species. PXR protein sequences from a selected set of different species were obtained from the UniProt and Ensembl databases, including e.g., human (*Homo sapiens*), zebrafish (*Danio rerio*) and mouse (*Mus musculus*). A multiple sequence alignment (MSA) was produced in Muscle (EMBL-EBI), using the hakePXR-hinge-LBD sequence cloned and sequenced in this thesis. The MSA was then visualized and edited in Jalview 2.11.2.2. The part of the MSA representing the hinge-region and the ligand binding domain (LBD) of PXR was used to create a maximum likelihood tree with maximum parsimony and bootstrap 1000 in MEGAX v.10.2.6.

3.5.2 *MSA - annotation of functional domains and ligand-binding residues*

Well annotated PXR protein sequences from human and zebrafish were obtained from UniProt and aligned with the hakePXR-hinge-LBD sequence obtained in this thesis. The MSA of human, hake, and zebrafish PXR protein sequences was produced in Clustal Omega (EMBL-EBI), then visualized and edited in Jalview 2.11.2.2. From the MSA, the hinge-region and LBD were identified and defined in the hake PXR sequence. Furtermore, the MSA visualizes the hinge-region and the LBD only, and not DBD, as these were the functional domains included in the partial PXR sequences used in this thesis. In addition, secondary structure (α-helixes and β-sheets), residues involved in ligand-binding and residues interacting with co-activator (SRC-1) were annotated based on previous studies of human PXR (Lichti-Kaiser, Brobst, Xu, & Staudinger, 2009; Lille-Langøy et al., 2015).

3.6 *Western blot assay*

3.6.1 *Sodium-dodecyl-sulfate polyacrylamide gel electrophoresis (SDS-PAGE)*

SDS-PAGE is a method used to separate proteins according to molecular size. Here, two gels were run: one for separation and visualization of total protein content in transfected COS-7 cells (Method 3.6.3), and one for verification of expression of the pCMX-GAL4-PXR-hinge-LBD fusion proteins in transfected COS-7 cells (Method 3.6.4).

To run an SDS-Page, protein samples are first mixed with a sample buffer containing β-mercaptoethanol and SDS, then denatured at 95℃. β-mercaptoethanol acts as a reducing agent and destroys the proteins tertiary structure by breaking disulfide bonds, and the anionic detergent SDS binds to the denatured protein creating a negatively charged polypeptide chain. The negative charge of the protein-SDS complexes allows migration through a polyacrylamide gel based on their molecular size, thereby separating the protein content.

3.6.2 *Preparation of cell lysate samples*

COS-7 cells were seeded in a 96-well plate and incubated at 37℃ with 5% CO_2 for 18-24 hours (Method 3.7.3). The next day, old medium was discarded, transfection mix with fresh cultivation medium was added, and the cells were further incubated at 37℃ with 5% CO_2 for 24 hours (Method 3.7.4). On the third day, old medium was discarded, and the cells were washed with 100 µL 1X PBS (pH 7.4) per well. Then, 20 µL lysis buffer (Table 13) was added to each well and the plate incubated on ice on a shaker for 5 min. Cell lysate was transferred from the wells into Eppendorf tubes and stored at -80℃.

3.6.3 *Total protein staining*

To separate and visualize total protein content from the transfected COS-7 cells a 1 mm thick polyacrylamide gel was casted. The polyacrylamide gel composed of a stacking gel and a 12% separation gel was made and set to polymerize. The gel was then transferred to an electrophoresis chamber, and the chamber was filled with 1X TGS buffer. Cell lysate samples were thawed on ice, then boiled at 95℃ for 5 min. 20 µL of each cell lysate sample was loaded into the wells on the gel. 5 µL Precision Plus Protein™ All Blue Prestained Protein Standards was loaded in one well and used as a molecular weight marker. The gel was run at

80V for 10 min, then 150V for 50 min. To visualize the separated protein content, the gel was transferred to a container and added InstantBlue™ Coomassie Protein Stain (Expedeon), then placed on a shaker at RT for overnight staining. The next day, excess stain was poured off and the gel was washed with ddH_2O. A ChemiDoc XRS+ (Bio-Rad) instrument was used to take a picture of the stained gel, visualizing the separated protein content.

3.6.4 *Western blotting*

Western blotting is a method where specific proteins separated by SDS-PAGE can be detected using antibodies. This method was used to verify the expression of the pCMX-GAL4-PXR-hinge-LBD fusion proteins in transfected COS-7 cells.

An SDS-PAGE was conducted as described in Method 3.6.3, and then used for Western blotting. A Mini Trans-Blot Electrophoretic Transfer Cell was used. First, the Western blot "sandwich" was assembled, which consisted of 2x sponges, 2x Whatman filter paper, 1x nitrocellulose membrane and the SDS-PAGE gel. All the components of the "sandwich" was submerged in cold 1X transfer buffer (TG), and then assembled in a specialized holder in the following order: sponge → paper → gel → membrane → paper → sponge. The holder with the "sandwich" was then placed in the electrophoresis chamber, two cooling units were added, and the chambre was filled with an appropriate volume of cold 1X TG buffer. The blot was run at 100V for 1 hour.

After the blotting was complete, the membrane was transferred to a container and blocked with 7% dry-milk in TBST at RT for 1 hour on a shaker. The TBST w/7% dry milk was then poured off and the membrane was washed with TBST. Primary antibody (anti-GAL4[DBD] antibody from mouse, Santa Cruz) was diluted 1:2000 in TBST with 1% milk and added to the membrane, and then incubated overnight on a shaker at 4℃. Excess antibody/TBST solution was then poured of, and the membrane was washed with TBST. Secondary antibody (anti-mouse IgG HRP antibody from sheep, GE healthcare) was diluted 1:2000 in TBST with 3% milk and added to the membrane and incubated on a shaker for 1 hour at RT. Excess antibody/TBST solution was poured off, and the membrane was washed with TBST. SuperSignal™ West Pico PLUS Chemiluminescent Substrate kit (Thermo Scientific) was used to visualize the pCMX-GAL4-PXR-hinge-LBD fusion proteins. The kits instruction manual was followed, and a substrate working solution was prepared by mixing equal parts of

the Luminol/Enhancer solution and Stable Peroxide solution. The substrate working solution was poured onto the membrane and incubated at RT for 5 min. A ChemiDoc XRS+ (Bio-Rad) was used to visualize and take pictures of the protein bands.

β-actin is a protein that is expressed in all eucaryotic cells, and was therefore used as a loading control. The blot treated with anti-GAL4[DBD] and anti-mouse HRP antibodies was washed with TBST, before the new primary antibody (anti-β-actin from mouse, Abcam) was diluted 1:10 000 in TBST with 1% milk and added to the membrane. The membrane was then incubated on a shaker for 1 hour at RT. Excess antibody/TBST solution was poured of, and the membrane was washed with TBST. Secondary antibody (anti-mouse HRP, sheep) was diluted 1:2000 in TBST with 3% milk and added to the membrane and incubated on a shaker for 1 hour at RT. Excess antibody/TBST solution was poured off and the membrane was washed with TBST. SuperSignal™ West Pico PLUS Chemiluminescent Substrate kit was used as previously described, and the β-actin protein bands were visualized with a ChemiDoc XRS+ (Bio-Rad).

3.7 *Luciferase reporter gene assay (LRA) – receptor ligand activation*

3.7.1 *Principle of the LRA*

Luciferase reporter gene assay (LRA) was used to measure ligand-induced activation of hakePXR, humanPXR and zebrafishPXR. COS-7 cells were transfected with a reporter-plasmid ((MH100)x4tkluc) which contains the reporter-gene luciferase, a pCMX-GAL4-PXR-hinge-LBD receptor-plasmid, and a pCMV-β-Gal normalization plasmid. Upstream GAL4-activation sequences (UAS) in the promoter region of the reporter-plasmid regulates the expression of the luciferase gene. When a ligand binds to the expressed pCMX-GAL4-PXR-hinge-LBD receptor protein it undergoes conformational changes which activates the GAL4-domain. The fusion protein then binds to the UAS and induces expression of the luciferase reporter-gene. The luciferase enzyme catalyzes luciferin into oxyluciferin and light (550 nm – 570 nm), making it possible to detect and quantify the ligand-induced activation of the receptor-protein (Figure 11). The normalization plasmid is constitutively expressing β-galactosidase, an enzyme that catalyzes ONPG into galactose and ONP. The product appears yellow, and absorbance can be measured at 420 nm and quantified as β-galactosidase activity.

β-galactosidase activity is then used to normalize the transfection efficiency of COS-7 cells, by dividing measured luciferase activity on measured β-gal-activity.

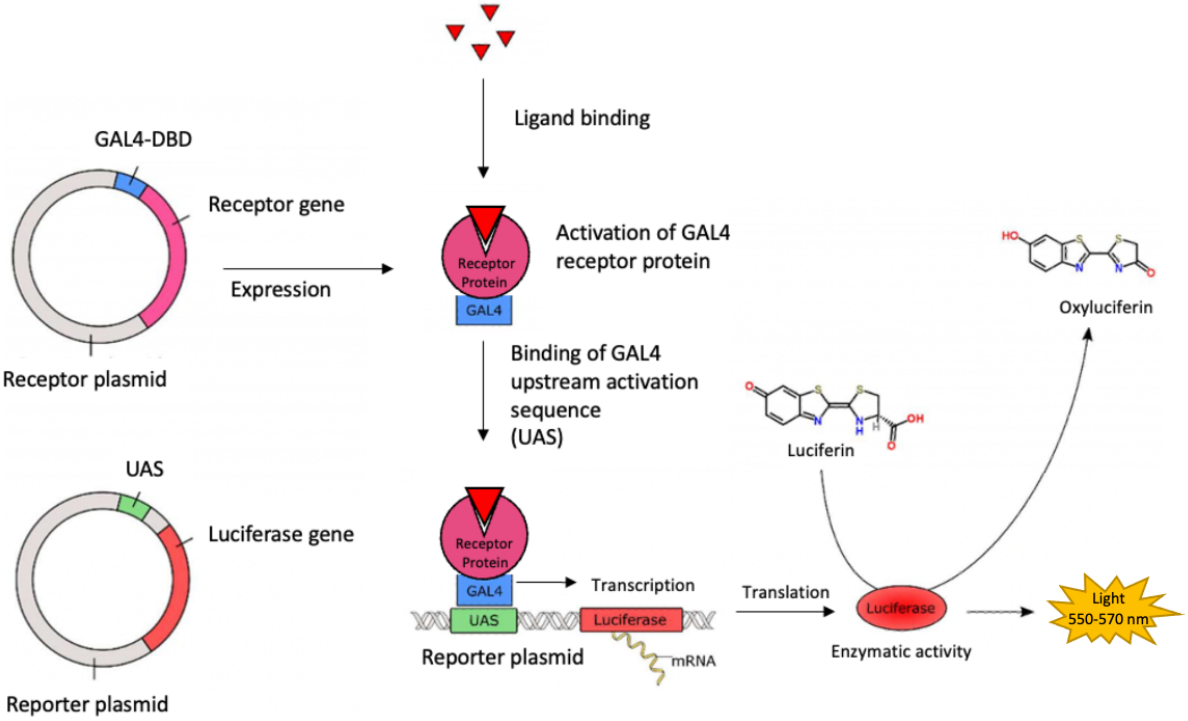

Figure 11. Illustration of the principle behind the luciferase reporter gene assay. Receptor- and reporter-plasmids are transfected into COS-7 cells. The receptor plasmid is constitutively expressed, and when a ligand binds to the receptor protein it undergoes a conformational change which activates the GAL4-DBD domain. GAL4-DBD then binds to UAS and induces expression of the reporter-gene luciferase. Luciferase catalyzes the transformation of luciferin to oxyluciferin and quantifiable light. The illustration is adapted from Madsen (2016).(Madsen, 2016)

3.7.2 *Cultivation of COS-7 cells*

Aliquots of COS-7 cells in freezing medium were stored in a liquid nitrogen tank. A vial of COS-7 cells was retrieved from storage, quickly thawed, and added 10 mL cultivation medium (DMEM-10%FBS). The cell/medium mix was centrifuged at 500 rpm and RT for 5 min. The supernatant was removed, and the pellet was resuspended in 10 mL fresh cultivation medium. Cells were then seeded in a 10 cm petri dish and incubated at 37℃ with 5% CO_2. Cell growth was monitored with a Leica DM IL inverted microscope, and at a confluency of 70-90% the cells were split. First, the old medium was removed, and the cells were washed with 1X PBS (pH 7.4) twice. Then, 1.5 mL Trypsin-EDTA (0.05% trypsin, 0.02% EDTA) was added, to allow cells to detach from the surface of the plate. After a 45 sec incubation at RT the trypsin was removed, and the cells were further incubated at 37℃ with 5% CO_2 for 5

min. Finally, cells were resuspended in cultivation medium, added to new plates in a 1:20 dilution with cultivation medium, and incubated at 37℃ with 5% CO_2.

3.7.3 *Seeding of COS-7 cells*

When the COS-7 cells reached a confluency of 70-90% the cells were detached from the plate and split as described above (Method 3.7.2). A 1:1 mix of resuspended cells and erythrosine B was prepared and cell density was determined by using a hemocytometer (Marienfield) with the Leica DM IL inverted microscope. The cell suspension was further diluted with cultivation medium before 100 µL of cell suspension (50 000 cells/mL) was seeded in each well of a 96-well plate. Cells were then incubated at 37℃ with 5% CO_2 for 18-24 hours.

3.7.4 *Transfection of COS-7 cells*

A transfection mix (Table 50) consisting of Opti-MEM I, plasmid mix (Table 49), and TransIT-LT1 was prepared and incubated at RT for 30 min. After incubation, the transfection mixture was added to DMEM-10% FBS. Old medium was discarded from the 96-well plate and 101 µL of the prepared transfection-DMEM mix was added to each well. Cells with transfection mix were then incubated at 37℃ with 5% CO_2 for 24 hours.

Table 49. Plasmid mix

Plasmid	Amount per well (ng)
(MH100)x4 tk luc	47.62
pCMV-β-Gal	47.62
pCMX-GAL4-hakePXR/humanPXR/zebrafishPXR-TL*	4.76

*Plasmid mixtures containing either the receptor plasmid pCMX-GAL4-hakePXR, pCMX-GAL4-humanPXR or pCMX-GAL4-zebrafishPXR-TL were prepared for the different experiments.

Table 50. Transfection mix

Components	Volume per well (µL)
Opti-MEM I	9.0
Plasmid mix (1000 ng/µL)	0.1
TransIT-LT1	0.2
DMEM-10% FBS	92.0

3.7.5 *Ligand Exposure*

Transfected COS-7 cells were exposed to three different ligands: clotrimazole, rifampicin and butyl 4-aminobenzoate. Ligands were dissolved in DMSO, and further serial diluted in phenol-red free cultivation medium (DMEM-10% FBS w/o phenol red) and DMSO. Serial dilution of the ligands was done in a deep 96-well plate with a dilution factor of 2 and 5, where ligand concentration declined from A to G. Well H contained cultivation medium and DMSO only and served as a solvent control without ligands. The serial dilutions were made in a 2X concentration of the final ligand concentrations. Old cultivation medium was discarded from the 96-well plate with transfected COS-7 cells, before 100 µL of fresh phenol-red free cultivation medium was added to each well. Then, 100 µL of the 2X ligand dilutions was added to their designated wells, giving a final 1X concentration of exposure ligands (Table 51). Cells exposed to ligands were then incubated at 37℃ with 5% CO_2 for 24 hours.

Table 51. Final concentrations of exposure ligands (µM) after serial dilution

Well	Clotrimazole	Rifampicin	Butyl 4-aminobenzoate
A	4.0	20.0	50.0
B	2.0	10.0	25.0
C	0.8	4.0	10.0
D	0.16	0.8	2.0
E	0.032	0.16	0.4
F	0.0064	0.032	0.08
G	0.00128	0.0064	0.016
H	0.0000001	0.0000001	0.0000001

3.7.6 *Lysis and luciferase activity measurements*

After 24 hours of exposure, the ligand medium was discarded from the plate. 125 µL cell lysis reagent (Table 21) was then added to each well of the 96-well plate, before the plate was incubated at RT for 30 min on a plate shaker. After incubation, 50 µL of cell lysate was transferred to the wells of a white 96-well luminescence plate and a clear 96-well absorbance plate used for luciferase activity and β-galactosidase absorbance measurements, respectively. 100 µL β-galactosidase reagent (Table 23) was added to each well of the clear 96-well absorbance plate, then the plate was incubated at RT until a bright yellow color emerged after

approximately 20 min. β-galactosidase absorbance was then measured at a wavelength of 420 nM in a Hidex Sense Microplate Reader. 100 µL luciferase reagent (Table 25) was added to each well of the white 96-well luminescence plate, and emitted light was immediately measured at 560 nm in a Hidex Sense Microplate Reader. The measurements were first processed in Microsoft Excel, where luciferase activity was divided on corresponding β-galactosidase absorbance to adjust for possible differences in transfection efficiency, thereby normalizing the measurements. Furthermore, the normalized luciferase activity was compared to the measurements from the control wells and fold change in luciferase activity was calculated. GraphPad Prism v.9.3.1 was used to produce a non-linear regression curve to visualize dose-response activation of luciferase activity induced by the different ligands.

3.8 *Cell viability assay*

A cell viability assay was performed to investigate the potential cytotoxic effect of the ligands used in the LRA on the COS-7 cells. CFDA-AM and Resazurin was used to measure cell membrane integrity and cell metabolism, respectively, as healthy cells would transform these chemicals into fluorescent compounds. COS-7 cells were seeded in a 96-well plate (Method 3.7.3), excluding a few wells that were kept empty for measurement of background signals, and incubated at 37℃ with 5% CO_2 for 18-24 hours. Old medium was then replaced with fresh cultivation medium, and cells were further incubated at 37℃ with 5% CO_2 for 24 hours. Most of the cells were exposed to the four highest concentrations of the ligands used in the LRA (Method 3.7.5), while some cells were exposed to Trition X-100 (0.5%) and served as positive controls for cell cytotoxicity. Exposed cells were incubated at 37℃ with 5% CO_2 for 24 hours. Exposure medium was then discarded, and cells were washed with 1X PBS (pH 7.4) before 100 µL of a resazurin/CFDA-AM reaction solution was added to each well. Cells were incubated at 37℃ with 5% CO_2 for 1 hour. Fluorescence signals were measured with the Hidex Sense Microplate Reader at 530/590 nm (excitation/emission) and 485/530 nm (excitation/emission) for resazurin and CFDA-AM, respectively. GraphPad Prism v.9.3.1 was used to visualize the changes in cell membrane integrity and cell metabolism.

4. Results

4.1 *Construction of pSC-B-hakePXR-hinge-LBD plasmids and pCMX-GAL4-hakePXR-hinge-LBD plasmids*

cDNA was synthesized from hake liver tissue, as described in Method 3.2, and was further used as a template for amplification of the hinge-LBD DNA sequence of *pxr* from hake. The cloned hake PXR sequences was subsequently used to construct the GAL4-based gene reporter system used to study ligand activation and ligand specificity for hake PXR.

4.1.1 *PCR amplification of the hakePXR-hinge-LBD DNA sequence*

Primers used to amplify the hinge-LBD-encoding DNA fragment of *pxr* from hake were designed as described in Method 3.3.1. The forward primers were constructed in order to align at the N-terminal side of the hinge-region, while the reverse primers aligned to the far C-terminal of the LBD (Primers shown in Table 37). The hakePXR-hinge-LBD fragment was amplified from liver cDNA by using PCR and separated and visualized on a 1% agarose gel. The primer pair MT2087 and MT2089 was used and produced a single bright DNA fragment at approximately 1100 bp (Figure 12), which is in accordance with the theoretical size of an amplified hakePXR-hinge-LBD (1062 bp) fragment.

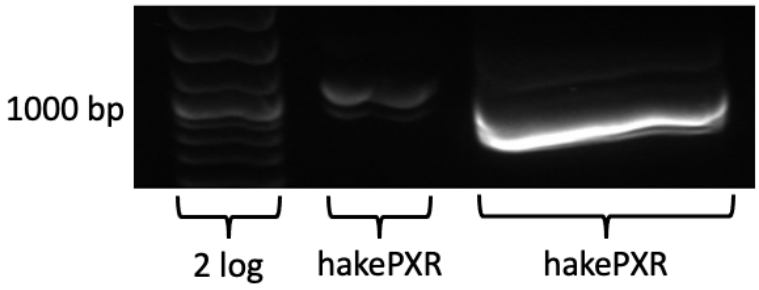

Figure 12. PCR amplification of hakePXR-hinge-LBD. The hinge-LBD DNA sequence of *pxr* from hake was amplified from liver cDNA using PCR with primer pair MT2087 and MT2089 (Table 37). From left to right, 3 µL and 50 µL PCR product was loaded on a 1% agarose gel to be separated and visualized. A 2-log DNA ladder was used as a molecular weight marker.

4.1.2 *Blunt-end PCR cloning of pSC-B-hakePXR-hinge-LBD plasmids*

The amplified hakePXR-hinge-LBD PCR product of interest (50 µL sample) were recovered from the agarose gel and purified as described in Method 3.3.3. The purified hakePXR-hinge-LBD PCR product was then ligated into the pSC-B cloning vector with blunt-end cloning, creating the pSC-B-hakePXR-hinge-LBD plasmid (Method 3.3.4). Plasmid construct was then transformed into competent *E. coli* cells, which were incubated overnight on LB-agar-ampicillin plates for blue-white colony screening with X-gal (Method 3.3.5). Six white bacteria colonies were randomly chosen and analyzed with colony PCR (Method 3.3.6). PCR products were separated on a 1% agarose gel to confirm the presence of pSC-B-hakePXR-hinge-LBD plasmids. As the primers used for the colony PCR (Table 40) bind to the pSC-B vector on each side of the hakePXR-hinge-LBD insert, bands slightly larger than the insert were expected. Figure 13 shows that most colonies examined had incorporated a fragment of approximately 1100 bp in size, which is in conformity with the expected size of the hakePXR-hinge-LBD (1062 bp). One of the colonies containing the pSC-B-hakePXR-hinge-LBD plasmid was chosen and plasmid purification (miniprep) was performed (Method 3.3.7.)

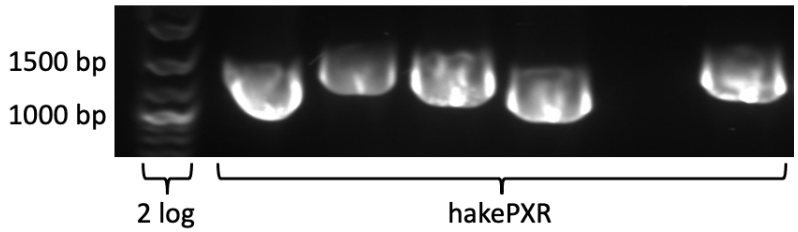

Figure 13. Colony PCR screening to confirm positive pSC-B-hakePXR-hinge-LBD transformants. To verify successful incorporation of hakePXR-hinge-LBD in the pSC-B vector after blunt-end cloning, colony PCR was performed. Six white colonies were randomly chosen from the blue-white colony screening, amplified using PCR, and separated and visualized on a 1% agarose gel. A 2-log DNA ladder was used as a molecular weight marker.

4.1.3 *Construction of pCMX-GAL4-hakePXR-hinge-LBD plasmids through restriction enzyme digestion*

To construct the final pCMX-GAL4-hakePXR-hinge-LBD plasmid, double digestion with restriction enzymes was performed (Method 3.4.1). Recognition sequences for the restriction enzymes EcoR1 and Nhe1 were introduced to the cloned hakePXR-hinge-LBD sequence through the primers used for the initial DNA amplification, while the previously constructed pCMX-GAL4-pbPPARG13 plasmid already contained their recognition sites. Therefore, EcoR1 and Nhe1 were used for digestion of both the pSC-B-hakePXR-hinge-LBD and the

pCMX-GAL4-pbPPARG13 plasmids, yielding compatible ends for ligation. SAP was added to the digested pCMX-GAL4-DBD vector to inhibit religation of the linearized DNA. The digested plasmids were separated and visualized on a 1% agarose gel. Figure 14 shows both the pSC-B-hakePXR-hinge-LBD plasmids (left) and the pCMX-GAL4-pbPPARG13 plasmid (right) after digestion. The lowest band of the pSC-B-hakePXR sample represent the hakePXR-hinge-LBD fragments (~1062 bp), while the highest band of the pCMX-GAL4-pbPPARG13 sample represents the pCMX-GAL4-DBD vector fragment (4500 bp). The bands corresponding to hakePXR-hinge-LBD and pCMX-GAL4-DBD fragments (red boxes) we excised from the agarose gel, and the DNA fragments were recovered and purified.

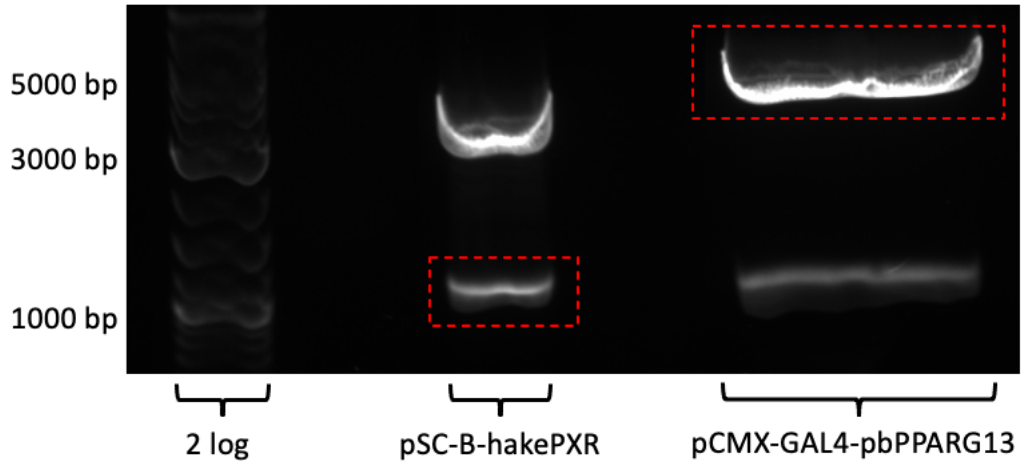

Figure 14. Restriction enzyme digestion of pSC-B-hakePXR-hinge-LBD plasmids and pCMX-GAL4-pbPPARG13 plasmid. The restriction enzymes EcoR1 (3´end) and Nhe1 (5´end) were used to digest both the pSC-B-hakePXR-hinge-LBD plasmids and the pCMX-GAL4-pbPPARG13 plasmid. The digested samples were separated and visualized on a 1% agarose gel to confirm that the digestion reactions were successful and to be able to isolate the DNA fragments of interest. The higher band (≥4300 bp) of the pSC-B-hakePXR samples represent undigested pSC-B-hakePXR-hinge-LBD plasmid and empty pSC-B vector, while the lower band (~1100 bp) represents the hakePXR-hinge-LBD fragment (red box). The higher band (~4500 bp) of the pCMX-GAL4-pbPPARG13 sample represents empty pCMX-GAL4-DBD vector (red box), while the lower band represents the pbPPARG13 fragment. A 2-log DNA ladder was used as a molecular weight marker.

Recovered DNA corresponding to the hakePXR-hinge-LBD fragment and empty pCMX-GAL4-DBD vector were mixed and ligated (Method 3.4.2). The ligation products were further used to transform competent *E. coli* cells (Method 3.4.3), which were incubated overnight on LB-agar-ampicilin plates. Colony PCR was performed to verify successful ligation of the pCMX-GAL4-hakePXR-hinge-LBD plasmid and transformation of the competent *E. coli* cells. Six colonies were randomly chosen from the transformants and amplified with PCR and primers given in Table 45. Colony PCR products were separated and visualized on a 1% agarose gel. Figure 15 shows the separated PCR products, where all

colonies produced DNA fragments of similar size (≥ 1100 bp). One colony were randomly selected and purified using miniprep (Method 3.3.7).

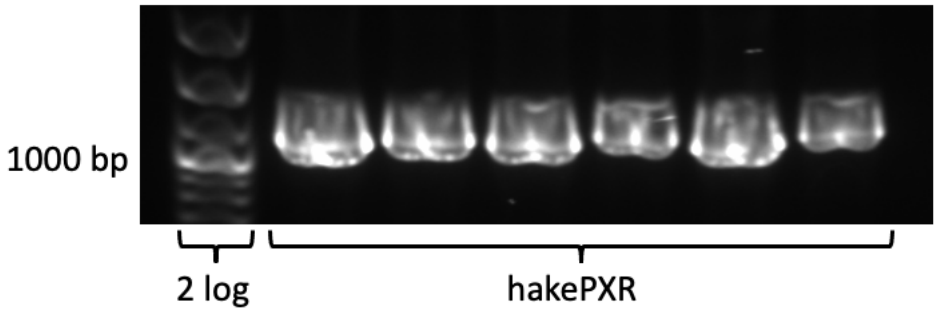

Figure 15. Colony PCR screening to confirm positive pCMX-GAL4-hakePXR-hinge-LBD transformants. Colony PCR and agarose gel electrophoresis were performed to verify the successful ligation of the pCMX-GAL4-hakePXR-hinge-LBD plasmids and incorporation in transformed bacteria colonies. Six colonies were randomly chosen from the transformants, and the hakePXR-hinge-LBD fragment was amplified using PCR and visualized on a 1% agarose gel. A 2-log DNA ladder was used as a molecular weight marker.

4.1.4 *Sanger sequencing of pCMX-GAL4-hakePXR-hinge-LBD plasmids*

Sequencing of the constructed pCMX-GAL4-hakePXR-hinge-LBD plasmid was performed to assure the incorporation of hakePXR-hinge-LBD into the pCMX-GAL4 vector in the correct reading frame, and to further examine the cloned hakePXR sequence, before the plasmid was utilized further in this thesis. The purified pCMX-GAL4-hakePXR-hinge-LBD plasmid sample was prepared for Sanger sequencing (Method 3.4.4), which was performed at the Department of Biological Science (UiB). By using specific forward and reverse primers (Table 46) the plasmid was sequenced in both directions. Sequencing results were aligned with the predicted hakePXR sequence obtained earlier through genome analysis (Eide et al., 2018, Sci Rep), and the results for the plasmid construct showed that the hakePXR-hinge-LBD sequence was fully incorporated in the pCMX-GAL4-DBD plasmid. Furthermore, a single point mutation of guanine to adenine was observed in the LBD of the sequenced hake PXR fragment, compared to the predicted hake PXR sequence. However, this was a silent mutation and would not have an impact on receptor function. The pCMX-GAL4-hakePXR-hinge-LBD plasmid construct was further used for the luciferase reporter gene assay.

4.2 *Bioinformatics*

4.2.1 *Phylogenetic analysis*

A phylogenetic analysis was performed to investigate the evolutionary relationship of hake PXR to PXR found in other species (Method 3.5.1). PXR protein sequences from various mammalian and teleost species were obtained from the UniProt and Ensembl databases, including human and zebrafish. Then, a MSA was produced, and based on the hinge-region and LBD of the aligned protein sequences, a maximum likelihood tree was made. Figure 16 shows the maximum likelihood tree, where the different PXR sequences are sorted based on their phylogenetic relations. As expected, PXR from hake was observed to have closest phylogenetic relationship to other teleost fishes, followed by amphibians and birds, while mammalian PXRs were clustered most distantly from hake.

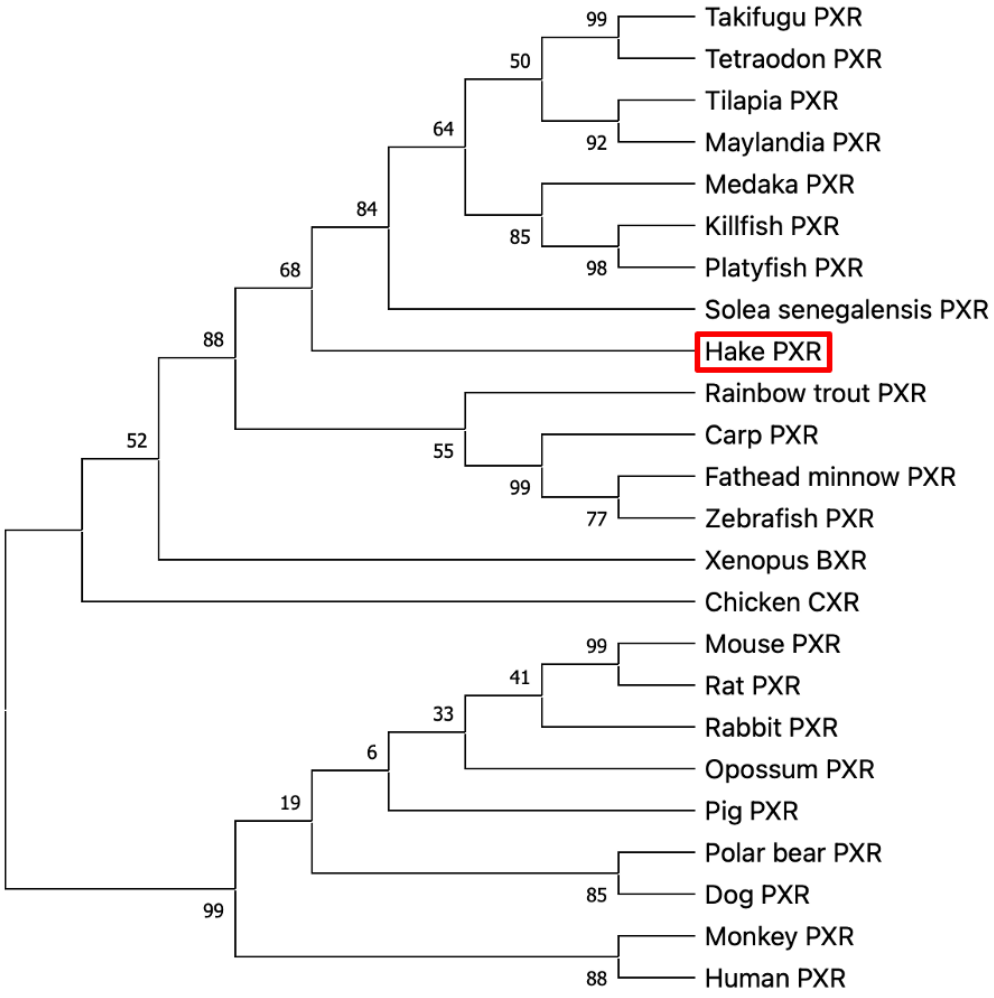

Figure 16. Phylogenetic tree analysis of PXR from different species. The maximum likelihood tree was made using maximum parsimony and bootstrap 1000 and represents the evolutionary relationship between hakePXR (red box) and PXR from different species. The phylogenetic analysis was constructed using the Muscle algorithm (EMBL-EBI) and MEGAX.

4.2.2 *Identifying the LBD and hinge-region and annotation of ligand-binding residues*

A MSA was made to compare important parts of the cloned hake PXR protein sequence with well characterized and annotated human and zebrafish PXR (Method 3.5.2). Sequence similarities were examined, and the hinge-region and LBD were located and identified in the hake PXR sequence based on the well annotated PXRs (Figure 17). When comparing the sequences, the LBD was moderately conserved with 46% (zebrafish) and 41% (hake) sequence identity compared to the human PXR-LBD. Furthermore, 12 α-helixes (including the ligand dependent activation function AF-2), 5 β-strands, residues involved in ligand binding, and residues involved in co-activator (SRC-1) interaction were predicted and annotated in the MSA based on previous studies of humanPXR (Lichti-Kaiser et al., 2009; Lille-Langøy et al., 2015). When assessing the amino acids known to be involved in ligand binding (red boxes), several substitutions have occurred cross species, including both conservative substitutions (e.g., F to Y) and non-conservative substitutions (e.g., L to S). Conversely, amino acids known to interact with co-activator (SRC-1) (green boxes) were highly conserved with no aa substitutions.

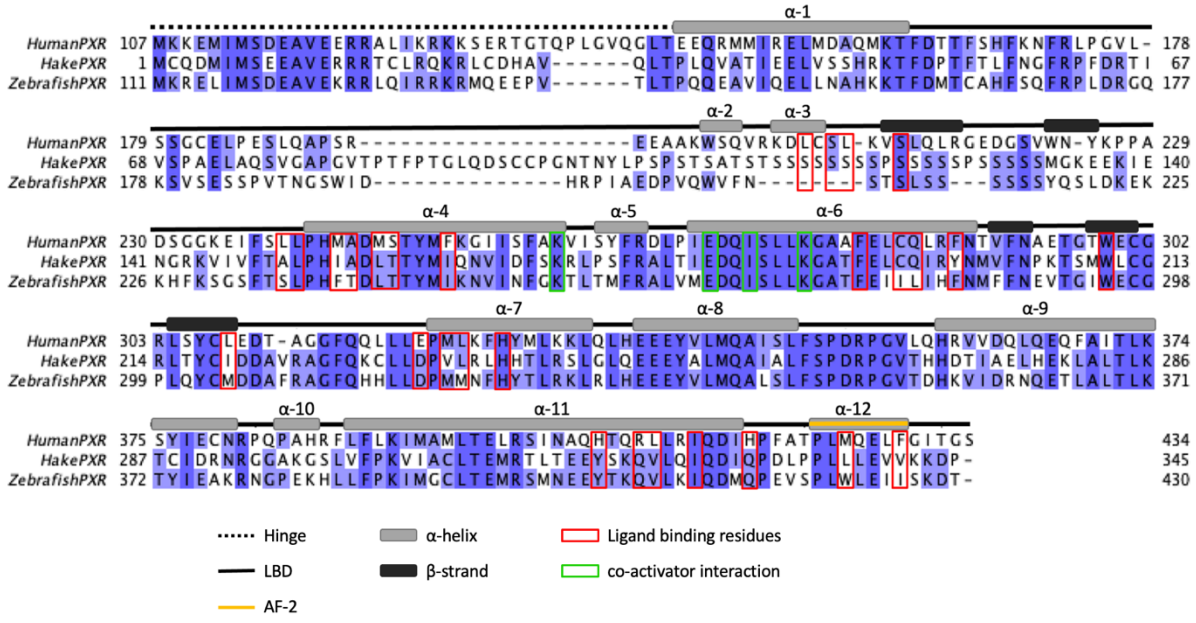

Figure 17. Multiple sequence alignment of humanPXR, hakePXR and zebrafishPXR. The PXR protein sequences were aligned in Clustal Omega and visualized in JalView. Blue colored residues correspond to amino acid percentage identity. The alignment includes annotations of the hinge-region, LBD (including AF-2), secondary structure (12 helixes and 5 β-strands), ligand binding residues (red), and residues interacting with co-activator (green) (Lichti-Kaiser et al., 2009; Lille-Langøy et al., 2015).

4.3 Assessment of plasmids used in COS-7 transfections and luciferase reporter gene assays

Concentration and integrity of plasmids used in western blot and LRA were assessed using spectrophotometry and agarose gel electrophoresis (Method 3.4.5). A Nanodrop 1000 instrument (Thermo Scientific) was used to measure both concentration and purity of the plasmid samples (Table 52). An absorbance ratio $A_{260nm/280nm}$ of approximately 1.8 or higher indicate that the DNA sample is pure, while lower ratios could indicate that protein or other contaminants are present. Absorbance ratio $A_{260nm/230nm}$ is a secondary measure of DNA purity, and a ratio ≥ 2.0 indicates that there are no co-purified contaminants in the sample.

Table 52. Plasmid DNA concentration and purity

Plasmid	Concentration (ng/µL)	$A_{260nm/280nm}$	$A_{260nm/280nm}$
(MH100)x4 tk luc	2656	1.93	2.39
pCMV-β-Gal	2484	1.94	2.34
hakePXR	2150	1.95	2.36
humanPXR	3151	1.94	2.36
zebrafishPXR-TL	2246	1.93	2.37

Agarose gel electrophoresis was performed to examine plasmid conformation, as it affects transfection efficiency into cells. Plasmids with supercoiled conformation was preferred as they are assumed to be more efficiently transfected into COS-7 cells. Figure 18 shows migration of the plasmids in the agarose gel, and most plasmids appear to have a supercoiled conformation.

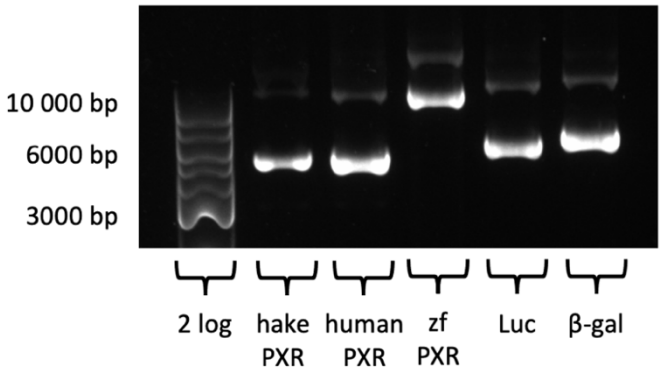

Figure 18. Agarose gel electrophoresis of plasmids used for western blotting and LRA. 200 ng of each plasmid sample was separated on a 1% agarose gel to examine plasmid conformation. hakePXR, humanPXR, zebrafishPXR (zfPXR), (MH100)x4 tk luc, and pCMV-β-Gal plasmid conformation was assessed. A 2-log DNA ladder was used as a molecular weight marker.

4.4 *Confirmation of synthesis of pCMX-GAL4-PXR-hinge-LBD fusion proteins in transfected COS-7 cells.*

Total protein staining and Western blotting of COS-7 cells transfected with pCMX-GAL4-PXR-hinge-LBD expression plasmids were performed to verify the expression and synthesis of the fusion proteins (Method 3.6). COS-7 cells were lysed 24 hours after pCMX-GAL4-PXR-hinge-LBD transfection and stored at -80℃ until use. SDS-PAGE was conducted as described in Method 3.6.3, producing two parallel gels. One gel was used for total protein staining with Coomassie Brilliant Blue, visualizing the separation and protein content in the transfected COS-7 cells. From the total protein staining, a similar protein distribution in all samples were observed, and the separation of protein content across the gel appeared to be successful (Figure 19). The second gel was used for western blotting with anti-GAL4 antibodies antibodies (Method 3.6.4), to assess the synthesis of the pCMX-GAL4-PXR-hinge-LBD fusion proteins. The molecular weight (Mw) of the hakePXR, humanPXR and zfPXR was predicted to be 55.4 kDa, 54.8 kDa, and 54.4 kDa, respectively. From the western blot (Figure 19), cells transfected with the PXR expression plasmids were observed to produce fusion proteins that migrated and formed immunoreactive bands at their predicted Mw, while non-transfected cells did not produce bands at the predicted size. Both transfected and non-transfected cells were observed to produce bands corresponding to β-actin (loading control) at 42 kDa, and the bands were of approximately equal intensity. Moreover, this demonstrated that the transfected COS-7 cells produced the desired pCMX-GAL4-PXR-hinge-LBD fusion proteins.

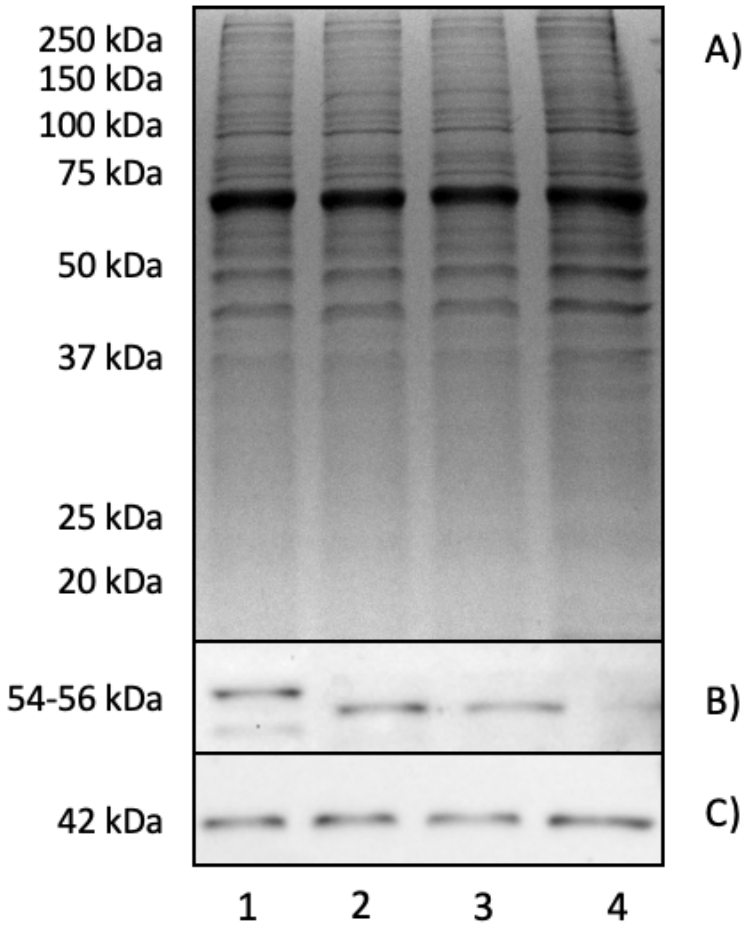

Figure 19. Verification of pCMX-GAL4-PXR-hinge-LBD fusion protein expression in transfected COS-7 cells. Total protein staining and Western blotting was performed to verify expression of pCMX-GAL4-PXR-hinge-LBD fusion proteins in transfected COS-7 cells. Wells were loaded from left to right with 1) hakePXR (55.4 kDa); 2) humanPXR (54.8 kDa); 3) zfPXR (54.4 kDa); and 4) non-transfected control. A) Total protein staining of SDS-PAGE with Coomassie Brilliant Blue. B) Western blot treated with anti-GAL4[DBD] antibody from mouse (primary) and anti-mouse IgG HRP antibody from sheep (secondary) to visualize the fusion proteins. C) Western blot treated with anti-β-actin from mouse (primary) and anti-mouse IgG HRP antibody from sheep (secondary) to visualize β-actin proteins at 42 kDa. SuperSignal™ West Pico PLUS Chemiluminescent Substrate kit was used to visualize the immunoreactive bands.

4.5 *Luciferase reporter gene assay (LRA)*

To investigate potential ligand-binding properties and activation of the cloned pCMX-GAL4-hakePXR-hinge-LBD plasmid, luciferase reporter gene assays were performed (Method 3.7). LRA was performed in triplicates at three separate occasions, to produce an average fold activation and persistent readings. As humanPXR and zebrafishPXR (zfPXR) ligand-binding properties are well characterized, LRA of these receptors were performed parallel to the assays of hakePXR as comparisons. Three compounds which are used in different pharmaceuticals and are known model ligands for PXR activation were selected for testing in the assays: clotrimazole, rifampicin, and butyl 4-aminobenzoate.

4.5.1 *Receptor ligand activation*

Normalized luciferase activity was calculated as fold change in receptor activation, and dose-response curves were made to illustrate receptor ligand activation (Figure 20). Lowest observed effect concentration (LOEC), maximum fold activation (E_{max}), and p-value are indicated in Table 53. EC_{50} values were not calculated as no clear activation plateaus were reached.

For hakePXR, clotrimazole produced a significant ($p<0.05$) activation of the receptor, while for rifampicin and butyl 4-aminobenzoate no significant activation was induced. A maximum fold activation (E_{max}) in luciferase activity of 6.4 was produced by clotrimazole at 4 μM. For humanPXR, only rifampicin induced a significant activation of the receptor, with measured E_{max} of 3 at 20 μM. For zfPXR, all three ligands produced activation of the receptor, however, rifampicin did not produce a significant activation. Clotrimazole produced the highest activation levels of zfPXR with an E_{max} of 23.8 at 4 μM, followed by butyl 4-aminobenzoate which produced an E_{max} of 4.7 at 50 μM.

Figure 21 visualizes a comparison of the different dose-response curves produced for each of the three ligands. By comparing the activation curves and assessing LOEC, clotrimazole shows a higher potency and efficacy for activation of zfPXR than of hakePXR, while humanPXR activation was not induced. Accordingly, rifampicin presents a higher potency for activation of humanPXR, but similar efficacy for activation of humanPXR and zfPXR. Butyl 4-aminobenzoate presents highest potency and efficacy for activation of zfPXR.

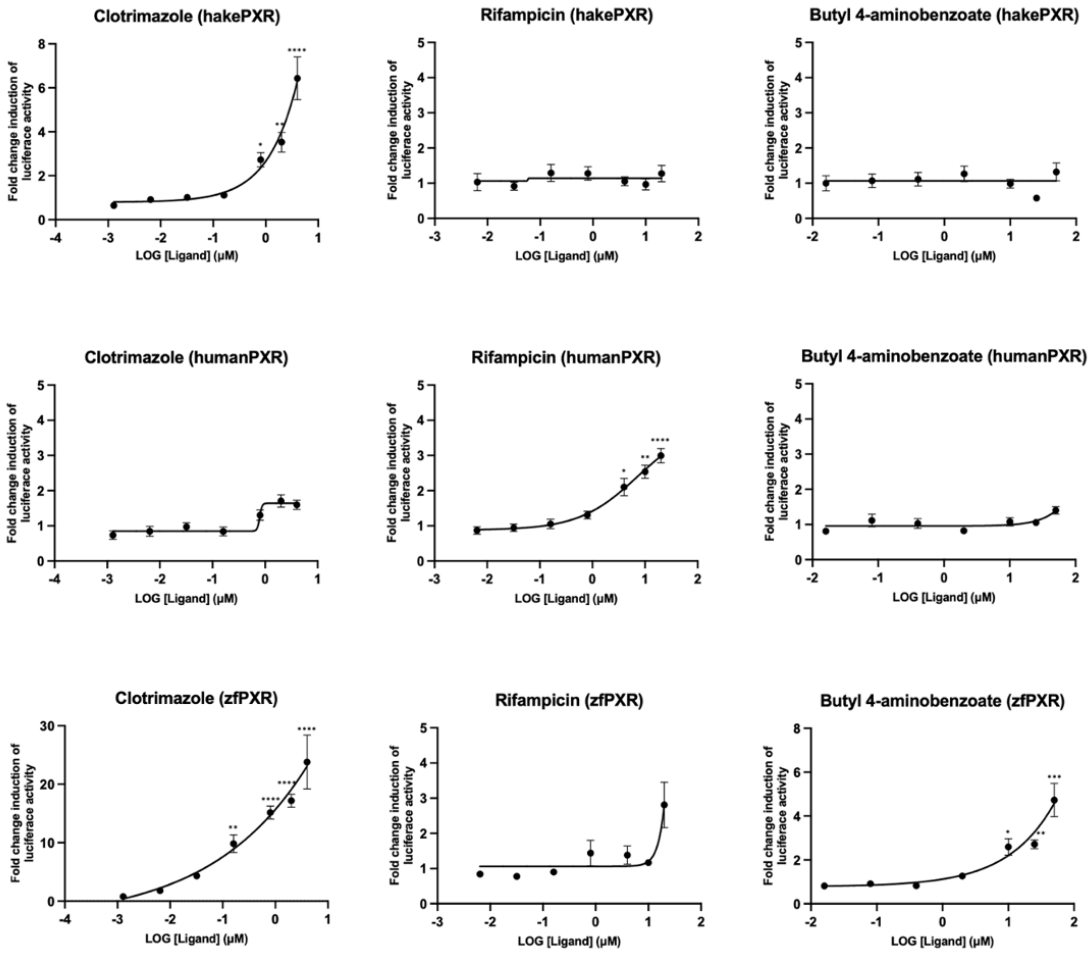

Figure 20. Ligand activation of pCMX-GAL4-hakePXR/humanPXR/zebrafishPXR-TL by clotrimazole, rifampicin, and butyl 4-aminobenzoate. COS-7 cells transfected with PXR receptor plasmid, reporter plasmid and normalization plasmid were exposed to serial diluted concentrations of clotrimazole, rifampicin and butyl 4-aminobenzoate. PXR activation is shown as relative fold change in luciferase activity compared to DMSO (0.2%) solvent control. Each point is average activation of triplicate measurements obtained from three separate experiments, with mean standard error bars (SEM). The dose-response curves were created in GraphPad Prism v.9.3.1. Statistical significance was calculated by using Kruskal-Wallis test with Dunn´s multiple comparisons test, and is indicated with *=p≤0.05, **=p≤0.01, ***=p≤0.001, ****=p≤0.0001.

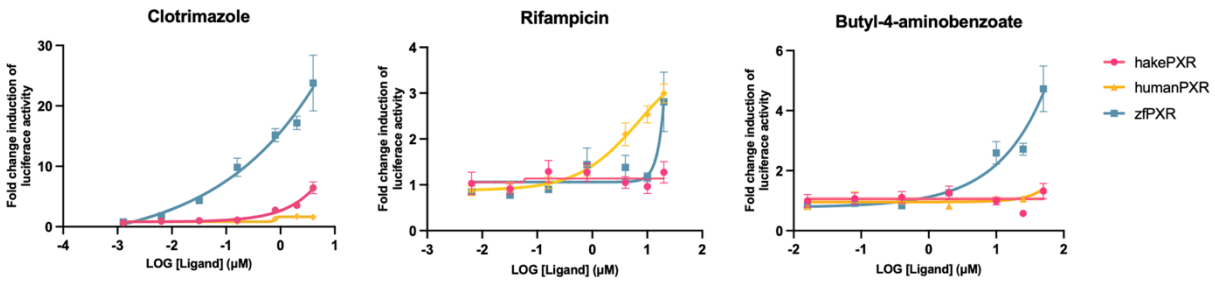

Figure 21. Comparison of dose-response curves illustrating ligand activation of hakePXR, humanPXR and zfPXR. Transfected COS-7 cells were exposed to clotrimazole, rifampicin and butyl 4-aminobenzoate, and PXR activation are shown as relative fold change in luciferase activity compared to DMSO (0.2%) solvent control. Each point is average activation of triplicate measurements obtained from three separate experiments, with mean standard error bars (SEM). Receptor activation by each ligand is compared, where hakePXR, humanPXR and zfPXR activation are indicated by pink, yellow and blue curves, respectively. The dose-response curves were created in GraphPad Prism v.9.3.1.

Table 53. Lowest observed effect concentration (LOEC), maximum fold activation (E_{max}) and statistical significance (p-value) for ligands used in LRA. LOEC (µM), E_{max} and p-value were calculated in GraphPad Prism v.9.3.1. p-value was calculated using Kruskal-Wallis test with Dunn´s multiple comparisons test.

Receptor	Agonist	LOEC (µM)	Maximum fold activation (E_{max})	p-value
hakePXR	Clotrimazole	0.8	6.4	<0.0001
hakePXR	Rifampicin	-	1.3	0.4299
hakePXR	Butyl 4-aminobenzoate	-	1.3	0.1933
humanPXR	Clotrimazole	-	1.7	<0.0001
humanPXR	Rifampicin	4.0	3.0	<0.0001
humanPXR	Butyl 4-aminobenzoate	-	1.4	0.0033
zfPXR	Clotrimazole	0.16	23.8	<0.0001
zfPXR	Rifampicin	-	2.8	0.0333
zfPXR	Butyl 4-aminobenzoate	10	4.7	<0.0001

4.5 *Cell viability results*

To monitor the potential cytotoxic effect of the ligands used in the LRA, a cell viability assay was performed with the COS-7 cells (Method 3.8). CFDA-AM and Resazurin was used to measure cell membrane integrity and cell metabolism, respectively. The cell viability assay was performed parallel with LRA, and the COS-7 cells were treated with the four highest exposure concentrations from each of the three ligands used: clotrimazole (4 µM, 2 µM, 0.8 µM, and 0.16 µM), rifampicin (20 µM, 10 µM, 4 µM, and 0.8 µM), and butyl 4-aminobenzoate (50 µM, 25 µM, 10 µM, and 2 µM). Cells treated with Triton X-100 (0.5%) served as positive controls for cell cytotoxicity. No significant decrease ($p<0.05$) in cell membrane integrity or cell metabolism was observed for any of the three exposure ligands (Figure 22).

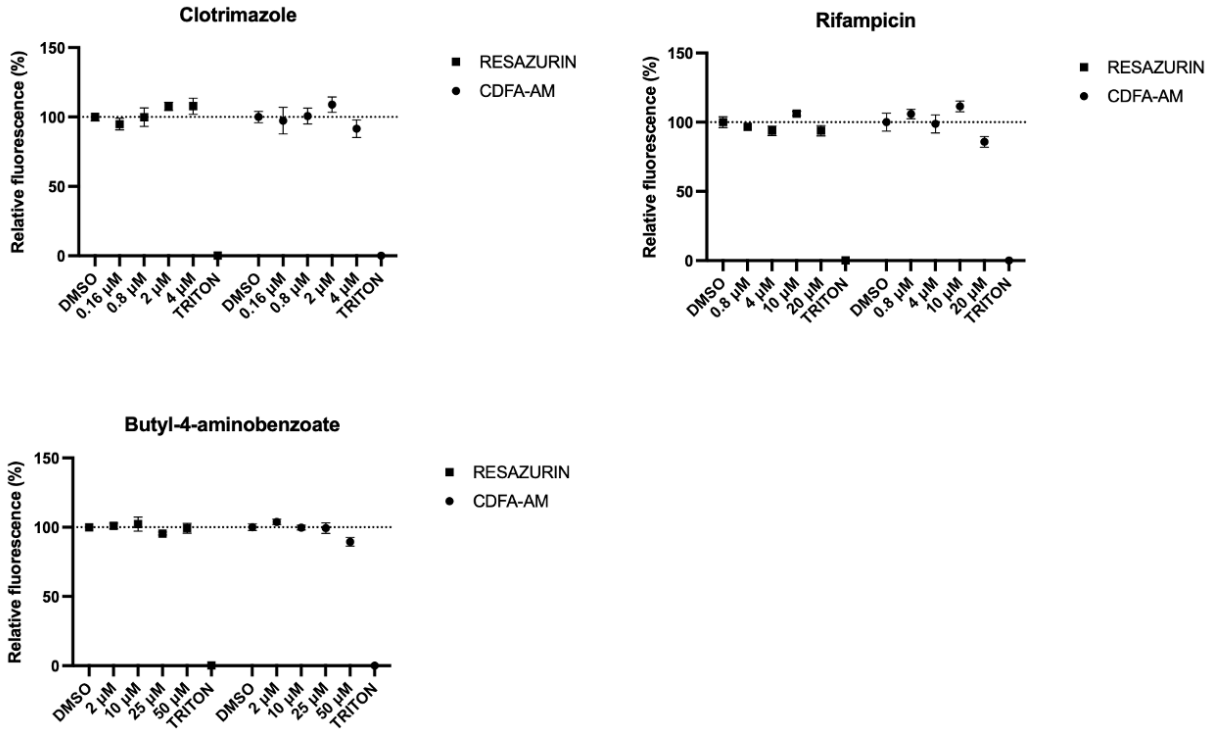

Figure 22. Cell viability assay of COS-7 cells. To investigate any cytotoxic effects of clotrimazole, rifampicin and butyl 4-aminobenzoate on COS-7 cells, a cell viability assay was performed. Cells were treated with the four highest exposure concentrations used in the LRA for each of the three ligands. 0.5% Triton X-100 was used as a positive control for cytotoxicity. The stippled line represents the solvent control, which was comprised of DMEM with 0.2 % DMSO. Circular dots represent change in membrane integrity (CFDA-AM) and squares represent change in cell metabolism (resazurin). Statistical significance was calculated in GraphPad Prism v.9.3.1 by using Kruskal-Wallis test with Dunn´s multiple comparisons test.

5. Discussion

The focus of this thesis has been to characterize PXR from European hake, concerning its primary structure, phylogeny, and ligand activation capabilities with exogenous compounds. PXR from other species has been observed to be activated by a great variety of xenobiotics, including rifampicin, clotrimazole, and butyl 4-aminobenzoate, displaying their properties as a xenosensor. As an xenosensor, PXR regulates the transcription of a battery of detoxification enzymes as a response to recognition and binding to chemical stressors. Thus, assessing the potential for xenobiotics to bind the PXR in European hake can provide more insight into the function and role of this receptor in this species.

5.1 *Evolution of PXR*

PXR is associated with both endogenous and exogenous ligand binding, and it has been a focus of numerous studies involving the defense system of organisms due to its role as an xenosensor. Furthermore, due to accumulation of man-made compounds in the aquatic environment and their potential as ligands for stress-activated receptors, interest regarding NRs such as PXR in teleost fishes have emerged. Interestingly, a recent genome-mining study by Eide et al. (2018) demonstrated the independent losses of the PXR in several teleost species. Furthermore, while most of the teleost species belonging to the *Gadiformes* order lacked a PXR-encoding gene, the receptor was identified in European hake. The retainment of PXR in hake is suggested to be due to retention of an ancestral gene, while independent losses in most *Gadiformes* teleosts have occurred.

In this thesis a phylogenetic analysis of was performed to investigate the evolutionary relationship of hake PXR to PXR found in other species. PXR from various species was included in the analysis, including both human and zebrafish. As expected, PXR from hake was observed to have closest phylogenetic relationship to other teleost fishes, while mammalian PXR was clustered most distantly from hake. This suggests that diverse changes to the *pxr* gene have occurred in early evolution, as sequence similarity is more conserved amongst closely related species. The evolutionary divergence of the different PXR genes might also, to some extent, explain the species-specific ligand recognition and activation of PXR observed in different studies (Creusot et al., 2021; Milnes et al., 2008). The study by Creusot et al. (2021) showed that human- and zebrafish PXR exhibited different activation

profiles upon exposure to different ligands, where some compounds induced agonistic effects in both PXR species, but producing different efficacies and potencies for the two species. Additionally, some compounds were shown to only act as an agonist or antagonists for PXR from only one of the species, while other compounds acted as either an agonist or an antagonist in a species-specific manner.

Furthermore, several naturally occurring PXR variants have been identified in both human- and zebrafish, which has shown to affect the receptor function (Bainy et al., 2013; Lille-Langøy et al., 2018; Rana, Devi, Gourinath, Goswami, & Tyagi, 2016). Variants of the PXR gene from a single zebrafish was detected by Bainy et al. (2013), while Lille-Langøy et al. 2018 identified PXR variants from four different strains of zebrafish, which exhibited different activation-profiles when exposed to model compounds. The diversity in both presence and number of variants (homologs) of the *pxr* gene inn different species are suggested to be due to several genetically altering events, including two whole genome duplication (WGD) events in early vertebrate evolution, a third fish specific WGD event, gene loss, inversions and neo- and subfunctionalizations, and single nucleotide polimorphisms (SNPs) (Eide et al., 2021; Rana et al., 2016). Moreover, a more comprehensive and detailed phylogenetic study in combination with thorough functional analyses of European hake PXR is needed to gain more information governing evolutionary events of gain and loss of ligand-binding function and subsequent transcription of detoxification enzymes by PXR.

5.2 *Ligand induced activation of human-, hake-, and zebrafish PXR*

In this thesis, a luciferase-based reporter gene assay was established and used to quantify ligand-induced activation of receptor-proteins (PXR), and thereby obtaining ligand-activation profiles for hakePXR, humanPXR and zebrafishPXR. The luciferase reporter gene assay is based on a GAL4-UAS interaction system which is widely used for targeted gene expression (Busson & Pret, 2007; Hartley, Nutt, & Amaya, 2002; Liu et al., 2019; Umeda et al., 2013; Zhao et al., 2014), and some advantages of using the system includes: downstream gene expression levels are much higher with the UAS promoter than with endogenous tissue-specific promoters, and it is possible to induce targeted gene expression of any gene of interest (Yamada, Nagasaki, Suzuki, Hirano, & Imayoshi, 2020).

Furthermore, COS-7 cells were transfected with the pCMX-GAL4-hakePXR-hinge-LBD, pCMX-GAL4-humanPXR-hinge-LBD, and pCMX-GAL4-zebrafishPXR-hinge-LBD, and subsequently exposed to rifampicin, clotrimazole and butyl 4-aminobenzoate. The expression of the luciferase reporter-gene was measured trough luminescence and quantified as ligand-induced activation of the PXR receptor, which allowed comparisons of activation profiles for the three PXR orthologs. The activation profiles for the three PXR orthologs are examined below.

5.2.1 *Assessment of ligand-induced activation profiles of the three PXR orthologs*

Transfected COS-7 cells were exposed to Rifampicin, due to its well-established role as an agonist for human PXR (Milnes et al., 2008). As expected, rifampicin was observed to induce activation of humanPXR, and it showed highest potency for binding of the human PXR. However, rifampicin exhibited similar efficacy for activation of zfPXR as for humanPXR, with an E_{max} of 2.8 and 3.0, respectively. Conversely, rifampicin did not induce any activation of hakePXR. These results are to some extent supported by the findings made by Creusot et al. (2021), as they reported activation of humanPXR by rifampicin. However, their findings also showed that rifampicin was unable to activate any response in zfPXR, which are not in concurrence with the findings in this thesis. Thus, the activation of zfPXR by rifampicin could be more closely investigated in future studies.

Furthermore, transfected COS-7 cells were also exposed to clotrimazole due to its known function as an agonist for PXR in zebrafish (Lille-Langøy et al., 2018; Milnes et al., 2008). As predicted, clotrimazole induced activation of zfPXR, and clearly displayed both highest potency and efficacy (E_{max} = 23.8) for induction of zfPXR compared to human- and hake PXR. Interestingly, this was the only compound that induce a significant activation of hakePXR (E_{max} = 6.4), while there was no significant activation of humanPXR. This suggests that the ligand binding properties resulting in species-specific activation from clotrimazole of PXR in zebrafish are conserved in the fellow teleost fish species European hake. This discovery is supported by the study by Milnes et al. (2018) that shows induction of PXR activity by clotrimazole in both zebrafish and fathead minnow. Furthermore, the findings made by Creusot et al. (2021) also highlights activation of PXR in zebrafish by clotrimazole, supporting the findings of this thesis. However, they also showed that humanPXR was activated by clotrimazole, although with lower potency and efficacy. The comparison study of

PXR activity by Lille-Langøy et al. (2015) shows that both human and polarbear PXR were activated by clotrimazole, further supporting the findings by Creusot et al. (2021). This indicates that humanPXR can be activated by clotrimazole, even though no significant activation was observed in this thesis.

Finally, COS-7 cells were exposed to butyl 4-aminobenzoate, which has previously shown to induce PXR activation in zebrafish (Lille-Langøy et al., 2018). Butyl 4-aminobenzoate induced a significant activation of zfPXR, with an E_{max} of 4.7 fold induction, while no activation in neither human- or hakePXR were detected. Lille-Langøy et al. (2018) investigated differences in PXR function in different strains of zebrafish, where PXR in three out of four strains were shown to be activated by butyl 4-aminobenzoate. Furthermore, the zebrafish strains exhibiting PXR activation by this compound included the TL strain used in this thesis, which supports the activation-profile produced for zfPXR. Furthermore, Lin et al. (2019) conducted a study about ligand-activated transcriptional activation in two human PXR variants, where neither of the two receptor homologs were activated by butyl 4-aminobenzoate (Lin et al., 2009), supporting the results in this thesis.

The highest exposure concentrations of each compound were chosen based on previous studies. The highest concentration of rifampicin used was 20 μM, as earlier studies have used exposure concentrations raging from 5 – 50 μM resulting in activation of human PXR (Creusot et al., 2021; Milnes et al., 2008). Furthermore, highest exposure concentrations of clotrimazole and butyl 4-aminobenzoate were set to 4 μM and 50 μM, respectively, as Lille-Langøy et al. (2018) published a study where activation profiles of zebrafish-TL PXR reached a plateau at lower concentrations than 4.5 μM clotrimazole and 50 μM butyl 4-aminobenzoate. However, neither hakePXR, humanPXR, nor zfPXR reached a plateau in their activation-profile when exposed to the three compounds. Additionally, a cell viability assay was performed to assess potential cytotoxic effects of the exposure compounds on COS-7 cells, where no significant decrease in cell viability was observed for either of the compounds. Thus, future studies could try to expose the transfected cells with higher concentrations of exposure compounds as an attempt to reach a plateau in PXR activation, which were not done in this thesis due to time limitations. Finally, the possibility that transfected COS-7 cells did not express the some of the functional GAL4-PXR-hinge-LBDs were assessed with western blotting. The blot confirmed synthesis of the three fusion proteins

in transfected COS-7 cells, which suggested that the activation profiles produced for the different PXR receptors were reliable.

5.3 *Differences in the PXR-LBD of human-, hake-, and zebrafish PXR that might impact ligand binding*

The hinge-region and LBD of the cloned hake PXR protein sequence was aligned with well characterized and annotated human and zebrafish PXR to investigate potential differences in their LBDs that could affect ligand binding. When comparing the sequences, the LBD was moderately conserved with 46% (zebrafish) and 41% (hake) sequence identity compared to the human PXR-LBD. This was to no surprise, as Bainy et al. (2013) have previously reported that the LBD in zebrafish PXR had a 44% sequence identity compared to human PXR-LBD. Furthermore, amino acids known to interact with co-activator (SRC-1) was annotated, where no substitutions were observed. This could indicate that once the receptor is bound by a ligand, its ability to interact with co-activator and subsequently induce transcription of target gene was intact in all three species. Conversely, when assessing amino acids known to be involved in ligand binding, several substitutions are observed, including both conservative- and non-conservative substitutions. Amino acid W299 has shown to be part of an aromatic cage, referred to as the π-trap, buried at the bottom of the LBP (Banerjee, Chai, Wu, Robbins, & Chen, 2016; Creusot et al., 2021). The hydrophobic π-trap is comprised of the three amino acids F288, W299, and Y306, and is an important structure for ligand binding (Creusot et al., 2021). The findings made by Banerjee et al. (2016) emphasizes the importance of the conserved W299, as it was proven to play a critical role in ligand binding and subsequent induction of target gene (CYP3A4). Interestingly, W299 and Y306 were conserved across all three examined PXR species, while a substitution of F288Y had occurred in the PXR protein sequence from hake. However, F288Y is a conservative amino acid substitution, and would most likely not impact the ligand binding properties of the π-trap structure in PXR from the European hake. Furthermore, as mentioned above there were several other substitutions of residues involved in ligand binding, which might be an explanation for the different activation-profiles observed for human-, hake- and zebrafish PXR. To assess the impact of these substitutions, a mutagenesis assay introducing specific SNPs to the protein sequences could be utilized in future studies.

5.4 *Conclusion*

In this study the nuclear receptor PXR, with known functional role as an xenosensor that regulates transcription of detoxification enzymes as response to chemical stress, was successfully cloned from European hake liver and sequenced. The sequenced hakePXR was further characterized regarding its phylogeny and primary structure, where hakePXR showed most closely phylogenetic relationship with other teleost species. Furthermore, an *in vitro* luciferace-based reporter gene assay was established to assess the ligand-binding properties and activation of hake. Various activation profiles of hakePXR were obtained, where only clotrimazole, the known agonist for zebrafish PXR, induced transcriptional activation of hakePXR. The changes to the *pxr* gene throughout evolution resulting in species-specific activation of the nuclear receptor, together with the several substitutions in amino acids with known ligand-binding properties, were suggested as a possible reason for the lack of hakePXR activation by rifampicin and butyl 4-aminobenzoate. In conclusion, these results suggests that PXR in European hake has maintained similar functional roles as observed in previous studies from e.g., human and zebrafish, regarding its role as an xenosensor that regulates transcription of response genes when bound by xenobiotics.

5.5 *Future perspectives*

In this study new information regarding PXR in European hake was produced. However, as very few studies involving PXR in European hake are available, the receptor should be more closely investigated with regards to both its structure, ligand activation, and physiological functions.

First, a more comprehensive phylogenetic analysis of PXR from different species should be performed to investigate potential evolutionary episodes of structure loss and changed ligand-binding function. Furthermore, expression and purification of recombinant protein and X-ray crystallography could provide important structural information, which may provide insight into ligand-binding properties of the receptor.

Continuing to investigate the ligand binding and activation of hakePXR should be of focus. The established luciferase reporter gene assay in this thesis could be used to further examine other compound's ability to transactivate hakePXR, including both xenobiotic and endobiotic

compounds. Furthermore, a mutagenesis assay where SNPs are introduced to amino acids known to be important for ligand binding could be applied. This would provide interesting insight to receptor function, regarding how ligand binding and subsequent transcriptional activation is affected.

Also, the assay established in this thesis is based on *in vitro* methods, which means that the receptor function might not appear identical *in vivo*, with regards to activation potency and efficacy observed for the compounds. To investigate PXR function in intact European hake, *in vitro* methods such as precision cut liver slices (PCLS) could be used. Finally, by exposing PCLS from European hake to known PXR agonists, one can study the transcriptional effect on biotransformation enzymes such as CYP3A and CYP1A.

7. List of References

Aranguren-Abadía, L., Lille-Langøy, R., Madsen, A. K., Karchner, S. I., Franks, D. G., Yadetie, F., . . . Karlsen, O. A. (2020). Molecular and Functional Properties of the Atlantic Cod (Gadus morhua) Aryl Hydrocarbon Receptors Ahr1a and Ahr2a. *Environmental Science & Technology, 54*(2), 1033-1044. doi:10.1021/acs.est.9b05312

Bainy, A. C. D., Kubota, A., Goldstone, J. V., Lille-Langøy, R., Karchner, S. I., Celander, M. C., . . . Stegeman, J. J. (2013). Functional characterization of a full length pregnane X receptor, expression in vivo, and identification of PXR alleles, in Zebrafish (Danio rerio). *Aquatic Toxicology, 142-143*, 447-457. doi:https://doi.org/10.1016/j.aquatox.2013.09.014

Banerjee, M., Chai, S. C., Wu, J., Robbins, D., & Chen, T. (2016). Tryptophan 299 is a conserved residue of human pregnane X receptor critical for the functional consequence of ligand binding. *Biochemical Pharmacology, 104*, 131-138. doi:https://doi.org/10.1016/j.bcp.2016.02.009

Blewett, T. A., Ransberry, V. E., McClelland, G. B., & Wood, C. M. (2016). Investigating the mechanisms of Ni uptake and sub-lethal toxicity in the Atlantic killifish Fundulus heteroclitus in relation to salinity. *Environmental Pollution, 211*, 370-381. doi:https://doi.org/10.1016/j.envpol.2016.01.002

Busson, D., & Pret, A.-M. (2007). GAL4/UAS Targeted Gene Expression for Studying Drosophila Hedgehog Signaling. In J. I. Horabin (Ed.), *Hedgehog Signaling Protocols* (pp. 161-201). Totowa, NJ: Humana Press.

Chen, X., Li, L., Cheng, J., Chan, L. L., Wang, D.-Z., Wang, K.-J., . . . Cheng, S. H. (2011). Molecular staging of marine medaka: A model organism for marine ecotoxicity study. *Marine Pollution Bulletin, 63*(5), 309-317. doi:https://doi.org/10.1016/j.marpolbul.2011.03.042

Chrencik, J. E., Orans, J., Moore, L. B., Xue, Y., Peng, L., Collins, J. L., . . . Redinbo, M. R. (2005). Structural Disorder in the Complex of Human Pregnane X Receptor and the Macrolide Antibiotic Rifampicin. *Molecular Endocrinology, 19*(5), 1125-1134. doi:10.1210/me.2004-0346

Creusot, N., Garoche, C., Grimaldi, M., Boulahtouf, A., Chiavarina, B., Bourguet, W., & Balaguer, P. (2021). A Comparative Study of Human and Zebrafish Pregnane X

Receptor Activities of Pesticides and Steroids Using In Vitro Reporter Gene Assays. *Frontiers in Endocrinology, 12*. doi:10.3389/fendo.2021.665521

Dai, Y.-J., Jia, Y.-F., Chen, N., Bian, W.-P., Li, Q.-K., Ma, Y.-B., . . . Pei, D.-S. (2014). Zebrafish as a model system to study toxicology. *Environmental Toxicology and Chemistry, 33*(1), 11-17. doi:https://doi.org/10.1002/etc.2406

De Marco, L., Sassera, D., Epis, S., Mastrantonio, V., Ferrari, M., Ricci, I., . . . Urbanelli, S. (2017). The choreography of the chemical defensome response to insecticide stress: insights into the Anopheles stephensi transcriptome using RNA-Seq. *Scientific Reports, 7*(1), 41312. doi:10.1038/srep41312

Dean, M., Hamon, Y., & Chimini, G. (2001). The human ATP-binding cassette (ABC) transporter superfamily. *Journal of Lipid Research, 42*(7), 1007-1017. doi:https://doi.org/10.1016/S0022-2275(20)31588-1

di Masi, A., Marinis, E. D., Ascenzi, P., & Marino, M. (2009). Nuclear receptors CAR and PXR: Molecular, functional, and biomedical aspects. *Molecular Aspects of Medicine, 30*(5), 297-343. doi:https://doi.org/10.1016/j.mam.2009.04.002

Eide, M., Rydbeck, H., Tørresen, O. K., Lille-Langøy, R., Puntervoll, P., Goldstone, J. V., . . . Karlsen, O. A. (2018). Independent losses of a xenobiotic receptor across teleost evolution. *Scientific Reports, 8*(1), 10404. doi:10.1038/s41598-018-28498-4

Eide, M., Zhang, X., Karlsen, O. A., Goldstone, J. V., Stegeman, J., Jonassen, I., & Goksøyr, A. (2021). The chemical defensome of five model teleost fish. *Scientific Reports, 11*(1), 10546. doi:10.1038/s41598-021-89948-0

Germain, P., Staels, B., Dacquet, C., Spedding, M., & Laudet, V. (2006). Overview of nomenclature of nuclear receptors. *Pharmacological reviews, 58*(4), 685-704.

Goldstone, J. V. (2008). Environmental sensing and response genes in cnidaria: the chemical defensome in the sea anemone Nematostella vectensis. *Cell Biology and Toxicology, 24*(6), 483-502. doi:10.1007/s10565-008-9107-5

Goldstone, J. V., Hamdoun, A., Cole, B. J., Howard-Ashby, M., Nebert, D. W., Scally, M., . . . Stegeman, J. J. (2006). The chemical defensome: Environmental sensing and response genes in the Strongylocentrotus purpuratus genome. *Developmental Biology, 300*(1), 366-384. doi:https://doi.org/10.1016/j.ydbio.2006.08.066

Hartley, K. O., Nutt, S. L., & Amaya, E. (2002). Targeted gene expression in transgenic Xenopus using the binary Gal4-UAS system. *Proceedings of the National Academy of Sciences, 99*(3), 1377-1382. doi:doi:10.1073/pnas.022646899

Information, N. C. f. B. (2022a). PubChem Compound Summary for CID 2482, Butyl 4-aminobenzoate. Retrieved from https://pubchem.ncbi.nlm.nih.gov/compound/2482

Information, N. C. f. B. (2022b). PubChem Compound Summary for CID 2812, Clotrimazole. Retrieved from https://pubchem.ncbi.nlm.nih.gov/compound/2812.

Information, N. C. f. B. (2022c). PubChem Compound Summary for CID 135398735, Rifampicin Retrieved from https://pubchem.ncbi.nlm.nih.gov/compound/135398735.

Kretschmer, X. C., & Baldwin, W. S. (2005). CAR and PXR: Xenosensors of endocrine disrupters? *Chemico-Biological Interactions, 155*(3), 111-128. doi:https://doi.org/10.1016/j.cbi.2005.06.003

Lichti-Kaiser, K., Brobst, D., Xu, C., & Staudinger, J. L. (2009). A Systematic Analysis of Predicted Phosphorylation Sites within the Human Pregnane X Receptor Protein. *Journal of Pharmacology and Experimental Therapeutics, 331*(1), 65. doi:10.1124/jpet.109.157180

Lille-Langøy, R., Goldstone, J. V., Rusten, M., Milnes, M. R., Male, R., Stegeman, J. J., . . . Goksøyr, A. (2015). Environmental contaminants activate human and polar bear (Ursus maritimus) pregnane X receptors (PXR, NR1I2) differently. *Toxicology and Applied Pharmacology, 284*(1), 54-64. doi:https://doi.org/10.1016/j.taap.2015.02.001

Lille-Langøy, R., Karlsen, O. A., Myklebust, L. M., Goldstone, J. V., Mork-Jansson, A., Male, R., . . . Goksøyr, A. (2018). Sequence Variations in pxr (nr1i2) From Zebrafish (Danio rerio) Strains Affect Nuclear Receptor Function. *Toxicological Sciences, 168*(1), 28-39. doi:10.1093/toxsci/kfy269

Lin, Y. S., Yasuda, K., Assem, M., Cline, C., Barber, J., Li, C. W., . . . Schuetz, E. G. (2009). The major human pregnane X receptor (PXR) splice variant, PXR.2, exhibits significantly diminished ligand-activated transcriptional regulation. *Drug Metab Dispos, 37*(6), 1295-1304. doi:10.1124/dmd.108.025213

Liu, R., Zeng, W., Tan, T., Chen, T., Luo, Q., Qu, D., . . . Xu, H. (2019). Insights into the regulatory characteristics of silkworm fibroin gene promoters using a modified Gal4/UAS system. *Transgenic Research, 28*(5), 627-636. doi:10.1007/s11248-019-00175-w

Madsen, A. K. (2016). *Kloning, karakterisering og ligandaktivering av aryl hydrokarbonreseptor 2 (AHR2) fra Atlanterhavstorsk (Gadus morhua).* The University of Bergen, Retrieved from http://hdl.handle.net/1956/11985

Miller, D. J., Hemmrich, G., Ball, E. E., Hayward, D. C., Khalturin, K., Funayama, N., . . . Bosch, T. C. G. (2007). The innate immune repertoire in Cnidaria - ancestral

complexity and stochastic gene loss. *Genome Biology, 8*(4), R59. doi:10.1186/gb-2007-8-4-r59

Milnes, M. R., Garcia, A., Grossman, E., Grün, F., Shiotsugu, J., Tabb Michelle, M., . . . Blumberg, B. (2008). Activation of Steroid and Xenobiotic Receptor (SXR, NR1I2) and Its Orthologs in Laboratory, Toxicologic, and Genome Model Species. *Environmental Health Perspectives, 116*(7), 880-885. doi:10.1289/ehp.10853

Nacci, D., Huber, M., Champlin, D., Jayaraman, S., Cohen, S., Gauger, E., . . . Gomez-Chiarri, M. (2009). Evolution of tolerance to PCBs and susceptibility to a bacterial pathogen (Vibrio harveyi) in Atlantic killifish (Fundulus heteroclitus) from New Bedford (MA, USA) harbor. *Environmental Pollution, 157*(3), 857-864. doi:https://doi.org/10.1016/j.envpol.2008.11.016

Pascussi, J.-M., Gerbal-Chaloin, S., Duret, C., Daujat-Chavanieu, M., Vilarem, M.-J., & Maurel, P. (2008). The Tangle of Nuclear Receptors that Controls Xenobiotic Metabolism and Transport: Crosstalk and Consequences. *Annual Review of Pharmacology and Toxicology, 48*(1), 1-32. doi:10.1146/annurev.pharmtox.47.120505.105349

Rana, M., Devi, S., Gourinath, S., Goswami, R., & Tyagi, R. K. (2016). A comprehensive analysis and functional characterization of naturally occurring non-synonymous variants of nuclear receptor PXR. *Biochimica et Biophysica Acta (BBA) - Gene Regulatory Mechanisms, 1859*(9), 1183-1197. doi:https://doi.org/10.1016/j.bbagrm.2016.03.001

Renaud, J. P., & Moras*, D. (2000). Structural studies on nuclear receptors. *Cellular and Molecular Life Sciences CMLS, 57*(12), 1748-1769. doi:10.1007/PL00000656

Sever, R., & Glass, C. K. (2013). Signaling by nuclear receptors. *Cold Spring Harbor perspectives in biology, 5*(3), a016709.

Sevior, D. K., Pelkonen, O., & Ahokas, J. T. (2012). Hepatocytes: The powerhouse of biotransformation. *The International Journal of Biochemistry & Cell Biology, 44*(2), 257-261. doi:https://doi.org/10.1016/j.biocel.2011.11.011

Steinberg, C. E. W. (2012). Arms Race Between Plants and Animals: Biotransformation System. In C. E. W. Steinberg (Ed.), *Stress Ecology: Environmental Stress as Ecological Driving Force and Key Player in Evolution* (pp. 61-106). Dordrecht: Springer Netherlands.

Thau, L., Asuka, E., & Mahajan, K. (2022). Physiology, Opsonization. In *StatPearls*. Treasure Island (FL): StatPearls Publishing

Timme-Laragy, A. R., Cockman, C. J., Matson, C. W., & Di Giulio, R. T. (2007). Synergistic induction of AHR regulated genes in developmental toxicity from co-exposure to two model PAHs in zebrafish. *Aquatic Toxicology, 85*(4), 241-250. doi:https://doi.org/10.1016/j.aquatox.2007.09.005

Timsit, Y. E., & Negishi, M. (2007). CAR and PXR: The xenobiotic-sensing receptors. *Steroids, 72*(3), 231-246. doi:https://doi.org/10.1016/j.steroids.2006.12.006

Umeda, K., Shoji, W., Sakai, S., Muto, A., Kawakami, K., Ishizuka, T., & Yawo, H. (2013). Targeted expression of a chimeric channelrhodopsin in zebrafish under regulation of Gal4-UAS system. *Neuroscience Research, 75*(1), 69-75. doi:https://doi.org/10.1016/j.neures.2012.08.010

Wada, T., Gao, J., & Xie, W. (2009). PXR and CAR in energy metabolism. *Trends in Endocrinology & Metabolism, 20*(6), 273-279. doi:https://doi.org/10.1016/j.tem.2009.03.003

Wang, W., Prosise, W. W., Chen, J., Taremi, S. S., Le, H. V., Madison, V., . . . Lesburg, C. A. (2008). Construction and characterization of a fully active PXR/SRC-1 tethered protein with increased stability. *Protein Engineering, Design and Selection, 21*(7), 425-433. doi:10.1093/protein/gzn017

Weikum, E. R., Liu, X., & Ortlund, E. A. (2018). The nuclear receptor superfamily: A structural perspective. *Protein Science, 27*(11), 1876-1892. doi:https://doi.org/10.1002/pro.3496

Yadetie, F., Karlsen, O. A., Eide, M., Hogstrand, C., & Goksøyr, A. (2014). Liver transcriptome analysis of Atlantic cod (Gadus morhua) exposed to PCB 153 indicates effects on cell cycle regulation and lipid metabolism. *BMC Genomics, 15*(1), 481. doi:10.1186/1471-2164-15-481

Yamada, M., Nagasaki, S. C., Suzuki, Y., Hirano, Y., & Imayoshi, I. (2020). Optimization of Light-Inducible Gal4/UAS Gene Expression System in Mammalian Cells. *iScience, 23*(9), 101506. doi:https://doi.org/10.1016/j.isci.2020.101506

Zhao, B., Kokoza, V. A., Saha, T. T., Wang, S., Roy, S., & Raikhel, A. S. (2014). Regulation of the gut-specific carboxypeptidase: A study using the binary Gal4/UAS system in the mosquito Aedes aegypti. *Insect Biochemistry and Molecular Biology, 54*, 1-10. doi:https://doi.org/10.1016/j.ibmb.2014.08.001

8. Appendix

8.1 *All amplified hakePXR-hinge-LBD DNA fragments*

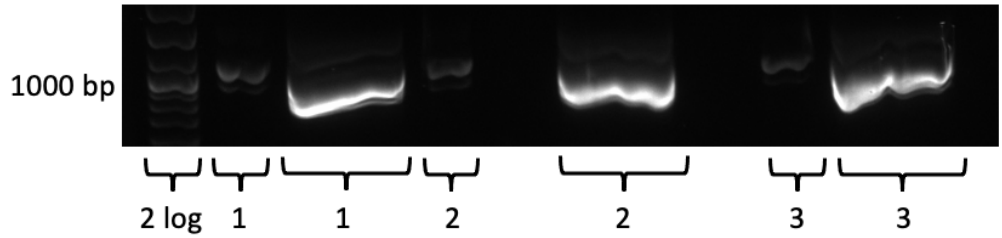

Figure 23. PCR amplification of hakePXR-hinge-LBD. The hinge-LBD DNA sequence of *pxr* from hake was amplified from liver cDNA using PCR, then 3µL and 50 µL of PCR products was loaded on a 1% agarose gel to be separated and visualized. The primer pair MT2087 and MT2089 (Table 37) were used for amplification of hakePXR-hinge-LBD in sample 1-3. A 2-log DNA ladder was used as a molecular weight marker.

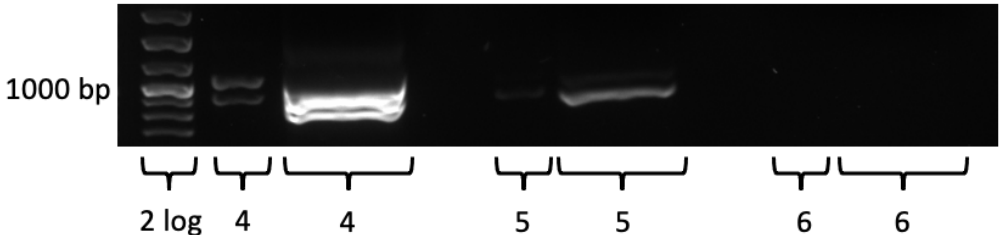

Figure 24. Amplification of hakePXR-hinge-LBD used to construct both pSC-B-hakePXR-hinge-LBD and pCMX-GAL4-hakePXR-hinge-LBD, sample 4-6. The hinge-LBD DNA sequence of *pxr* from hake was amplified from liver cDNA using PCR, then 3µL and 50 µL PCR product was loaded on a 1% agarose gel to be separated and visualized. The primer pair MT2087 and MT2094 (Table 37) were used for amplification of hakePXR-hinge-LBD in sample 4-6. A 2-log DNA ladder was used as a molecular weight marker.